

NAVAL POSTGRADUATE SCHOOL

Monterey, California



THESIS

REFRACTIVE CONDITION IN THE CARIBBEAN SEA AND ITS EFFECTS ON RADAR SYSTEMS

by

Douglas F. Seijas

September 1998

Thesis Advisor:

Kenneth L. Davidson

Co-Advisor:

David Jenn

Approved for public release; distribution is unlimited.

19981110 142

REPORT DOCUMENTATION PAGE

Form Approved
OMB No. 0704-0188

Public reporting burden for this collection of information is estimated to average 1 hour per response, including the time for reviewing instruction, searching existing data sources, gathering and maintaining the data needed, and completing and reviewing the collection of information. Send comments regarding this burden estimate or any other aspect of this collection of information, including suggestions for reducing this burden, to Washington headquarters Services, Directorate for Information Operations and Reports, 1215 Jefferson Davis Highway, Suite 1204, Arlington, VA 22202-4302, and to the Office of Management and Budget, Paperwork Reduction Project (0704-0188) Washington DC 20503.

1. AGENCY USE ONLY (Leave blank)

2. REPORT DATE
September 1998

3. REPORT TYPE AND DATES COVERED
Master's Thesis

4. TITLE AND SUBTITLE
REFRACTIVE CONDITION IN THE CARIBBEAN SEA AND ITS EFFECTS ON RADAR SYSTEMS

5. FUNDING NUMBERS

6. AUTHOR(S)
Seijas, Douglas F.

7. PERFORMING ORGANIZATION NAME(S) AND ADDRESS(ES)
Naval Postgraduate School
Monterey, CA 93943-5000

8. PERFORMING ORGANIZATION
REPORT NUMBER

9. SPONSORING / MONITORING AGENCY NAME(S) AND ADDRESS(ES)

10. SPONSORING / MONITORING
AGENCY REPORT NUMBER

11. SUPPLEMENTARY NOTES

The views expressed in this thesis are those of the author and do not reflect the official policy or position of the Department of Defense or the U.S. Government.

12a. DISTRIBUTION / AVAILABILITY STATEMENT

Approved for public release; distribution is unlimited.

12b. DISTRIBUTION CODE

13. ABSTRACT

Vertical gradients of pressure, temperature and humidity of the troposphere exert a strong influence over propagation of VHF, UHF, and SHF frequencies. These frequencies are associated with aircraft communications, radars and satellite communications, so it is important in military operations to collect precise and timely data from atmospheric conditions.

In this thesis programs from EREPS were used to assess refractive conditions in the Caribbean Sea against selected radar systems. Data given by SDS from radiosonde stations located in MS 43 and 44 were used as input for COVER and PROPR programs. Outputs from COVER are analyzed to find Optimal Altitude to Avoid Detection (OAAD) for a low-flying target. Outputs from PROPR using climatological data given by SDS and Optimal Altitude to Avoid Detection from COVER was used to verify OAAD against selected land- and ship-mounted radars operating in the Caribbean Sea. Finally, a system under development, TDROP is introduced in response to requirements for timely and exact data collection, in order to enhance the tactical data collection process.

14. SUBJECT TERMS

Refractive Conditions, Air Defense, Radar Systems

15. NUMBER OF PAGES

82

16. PRICE CODE

17. SECURITY CLASSIFICATION OF REPORT
Unclassified

18. SECURITY CLASSIFICATION OF THIS PAGE
Unclassified

19. SECURITY CLASSIFICATION OF ABSTRACT
Unclassified

20. LIMITATION OF ABSTRACT
UL

Approved for public release; distribution is unlimited

**REFRACTIVE CONDITION IN THE CARIBBEAN SEA AND ITS EFFECTS ON
RADAR SYSTEMS**

Douglas F. Seijas
Lieutenant Colonel, Venezuelan Air Force

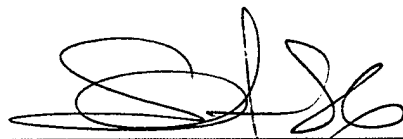
Submitted in partial fulfillment of the
requirements for the degree of

MASTER OF SCIENCE IN SYSTEM ENGINEERING

from the

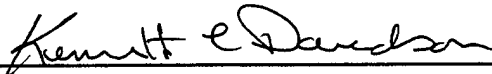
**NAVAL POSTGRADUATE SCHOOL
September 1998**

Author:

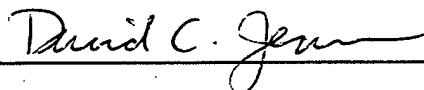


Douglas F. Seijas

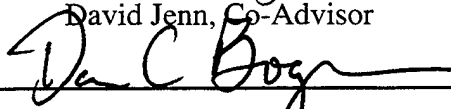
Approved by:



Kenneth L. Davidson, Thesis Advisor



David Jenn, Co-Advisor



Dan C. Boger, Chairman
Information Warfare Academic Group

ABSTRACT

Vertical gradients of pressure, temperature and humidity of the troposphere exert a strong influence over propagation of VHF, UHF, and SHF frequencies. These frequencies are associated with aircraft communications, radars and satellite communications, so it is important in military operations to collect precise and timely data from atmospheric conditions.

In this thesis programs from EREPS were used to assess refractive conditions in the Caribbean Sea against selected radar systems. Data given by SDS from radiosonde stations located in MS 43 and 44 were used as input for COVER and PROPR programs. Outputs from COVER are analyzed to find Optimal Altitude to Avoid Detection (OAAD) for a low-flying target. Outputs from PROPR using climatological data given by SDS and Optimal Altitude to Avoid Detection from COVER was used to verify OAAD against selected land- and ship-mounted radars operating in the Caribbean Sea. Finally, a system under development, TDROP is introduced in response to requirements for timely and exact data collection, in order to enhance the tactical data collection process.

TABLE OF CONTENTS

I.	INTRODUCTION.....	1
II.	SCENARIO.....	3
	A. GEOGRAPHICAL REGION.....	4
	B. CLIMATOLOGY.....	5
	C. ATMOSPHERIC CONDITIONS.....	7
III.	EFFECTS OF THE ATMOSPHERE ON ELECTROMAGNETIC WAVES PROPAGATION.....	11
	A. EM WAVE PROPAGATION.....	11
	B. ATMOSPHERIC INFLUENCE AND INDEX OF REFRACTION.....	12
	C. STANDARD AND REFRACTIVE GRADIENTS.....	14
	D. TRAPPING LAYERS AND DUCTS.....	17
IV.	RADAR SYSTEMS.....	19
	A. LAND-BASED RADAR SYSTEMS.....	22
	1. TPS-70.....	23
	2. Falcon.....	23
	3. Giraffe.....	24
	B. SHIP-MOUNTED RADAR SYSTEMS.....	24
	1. SPS-49.....	25
	2. RAN-10S.....	26
	3. Sea Tiger.....	26

V.	DATA ANALYSIS AND RESULT.....	27
A.	DATA ANALYSIS FOR LAND-BASED RADARS.....	29
1.	Curacao Zone.....	29
2.	Trinidad and Tobago Zone.....	35
B.	DATA ANALYSIS FOR SHIP-MOUNTED RADARS.....	41
1.	Antigua Zone.....	41
2.	Jamaica Zone.....	47
3.	Puerto Rico Zone.....	53
C.	SUMMARY OF RESULT.....	58
D.	CONSIDERATIONS FOR TACTICAL DATA COLLECTION.....	59
1.	Percent of Occurrence of Evaporation Ducts.....	59
2.	Enhancements in Tactical Data Collection (Tactical Dropsonde).....	61
VI.	CONCLUSIONS.....	65
	LIST OF REFERENCES.....	67
	INITIAL DISTRIBUTION LIST.....	69

LIST OF FIGURES

Figure 1. Representation of Marsden Squares.....	4
Figure 2. Stations in Marsden Squares 43 and 44.....	5
Figure 3. Radiosonde Stations in MS 43.....	8
Figure 4. Radiosonde Stations in MS 44.....	8
Figure 5. Relationship between ducts and M-value.....	18
Figure 6. Evaporation Duct Summary, Curacao zone.....	30
Figure 7. COVER output for TPS-70, Curacao zone.....	31
Figure 8. COVER output for Falcon, Curacao zone.....	32
Figure 9. COVER output for Giraffe, Curacao zone.....	32
Figure 10. PROPR output for TPS-70, Curacao zone.....	33
Figure 11. PROPR output for Falcon, Curacao zone.....	34
Figure 12. PROPR output for Giraffe, Curacao zone.....	34
Figure 13. Evaporation Duct Summary, Trinidad zone.....	36
Figure 14. COVER output for TPS-70, Trinidad zone.....	37
Figure 15. COVER output for Falcon, Trinidad zone.....	37
Figure 16. COVER output for Giraffe, Trinidad zone.....	38
Figure 17. PROPR output for TPS-70, Trinidad zone.....	39
Figure 18. PROPR output for Falcon, Trinidad zone.....	39
Figure 19. PROPR output for Giraffe, Trinidad zone.....	40
Figure 20. Evaporation Duct Summary, Antigua zone.....	42

Figure 21. COVER output for Sea Tiger, Antigua zone.....	43
Figure 22. COVER output for RAN-10S, Antigua zone.....	43
Figure 23. COVER output for SPS-49, Antigua zone.....	44
Figure 24. PROPR output for Sea Tiger, Antigua zone.....	45
Figure 25. PROPR output for RAN-10S, Antigua zone.....	45
Figure 26. PROPR output for SPS-49, Antigua zone.....	46
Figure 27. Evaporation Duct Summary, Jamaica zone.....	47
Figure 28. COVER output for Sea Tiger, Jamaica zone.....	48
Figure 29. COVER output for RAN-10S, Jamaica zone.....	48
Figure 30. COVER output for SPS-49, Jamaica zone.....	49
Figure 31. PROPR output for Sea Tiger, Jamaica zone.....	50
Figure 32. PROPR output for RAN-10S, Jamaica zone.....	50
Figure 33. PROPR output for SPS-49, Jamaica zone.....	51
Figure 34. Evaporation Duct Summary, Puerto Rico zone.....	52
Figure 35. COVER output for Sea Tiger, Puerto Rico zone.....	53
Figure 36. COVER output for RAN-10S, Puerto Rico zone.....	53
Figure 37. COVER output for SPS-49, Puerto Rico zone.....	54
Figure 38. PROPR output for Sea Tiger, Puerto Rico zone.....	55
Figure 39. PROPR output for RAN-10S, Puerto Rico zone.....	55
Figure 40. PROPR output for SPS-49, Puerto Rico zone.....	56

LIST OF TABLES

Table 1. Atmospheric conditions in the selected zones.....	9
Table 2. EREPS Refractive Gradients and Distance Relationship.....	16
Table 3. Basic types of Air Defense Systems.....	20
Table 4. Selected Radar Systems.....	21
Table 5. Specifications for land-based radar systems.....	22
Table 6. Specifications for ship-mounted radar systems.....	25
Table 7. Detection Distance Summary, Curacao.....	35
Table 8. Detection Distance Summary, Trinidad.....	41
Table 9. Detection Distance Summary, Antigua.....	46
Table 10. Detection Distance Summary, Jamaica.....	51
Table 11. Detection Distance Summary, Puerto Rico.....	57
Table 12. Percent of Occurrence of Evaporation Ducts.....	58
Table 13. TDROP operational and physical requirements.....	61

I. INTRODUCTION

The objective of this study is to evaluate the atmospheric effects on different land-based and ship-mounted radars to find the optimal climatological altitude for an aircraft penetrating a defense system on its way to an assigned target at the south of the Caribbean Sea.

Combat pilots in modern air operations must be familiar with the threats that can be found during the development of the assigned mission. So, they must be trained to apply tactics and measures that they may use to counterattack those threats, or even better to avoid being detected. One of those tactics is the exploitation of "natural" radar holes and ducts caused by atmospheric conditions. This anomalous propagation allows the propagation of energy to distances that exceed the nominal radar range, and are very common in coastal regions.

Information about abnormal propagation studies in the Caribbean Sea have all the evidence of being insufficient due to the fact that U.S. Military has been concentrated in areas like the Persian Gulf, Mediterranean Sea, and even the California Coast.

Some computer-based programs can be used in tactical operations to assess the effect of ducting conditions on the performance of selected

radar systems. In this study the computer code Engineer's Refractive Effects Prediction System (EREPS) provided not only the statistical atmospheric data to describe the features of the Caribbean Sea, but also the propagation model to predict the performance of selected radar systems.

Finally, the success in modern military operations depends on precise and timely tactical data collection, which includes atmospheric conditions leading to duct formation, so enhancements in methods of data collection are needed to meet operational requirements. TDROP is one of those methods of data collection, which is introduced in this study.

II. SCENARIO

The scenario considered in this study is located in the Caribbean Sea, where navies from different countries operate.

Six radar system were selected. Three of these radars are ship-mounted and the others are land-based, which can be used for coastal defense. The radars are in use by different countries in the region, such as Venezuela and Colombia. Also, the radars were produced by different manufacturers. In the following chapters a description of each system is given in more detail.

The suite of programs Engineer's Refractive Effects Prediction System (EREPS) was used in this study to predict the effects of atmospheric conditions caused by trapping and ducts, and to calculate Propagation Loss (L) in the selected region. EREPS is a system of individual stand-alone IBM/PC-compatible programs used to model the electromagnetic propagation of the lower atmosphere on proposed radar, electronic warfare, or communication systems. It was developed by the Naval Command, Control and Oceanic Center to account for effects from optical interference, diffraction, tropospheric scatter, refraction, evaporation and surface-based ducting, and water vapor absorption under horizontally structured atmospheric conditions [Ref. 1].

A. GEOGRAPHICAL REGION

The area of interest is located at the Marsden Squares (MS) 43 and 44. Each MS consists of a 10-degree by 10-degree square, as shown in Figure 1. The geographical region is located between the latitudes 10° N to 20° N and the longitudes 060° W and 080° W. It includes the Venezuela and Colombia north coasts, Puerto Rico, Dominican Republic, Haiti, Aruba, Curazao, Trinidad and Bonaire, and Jamaica, among others.

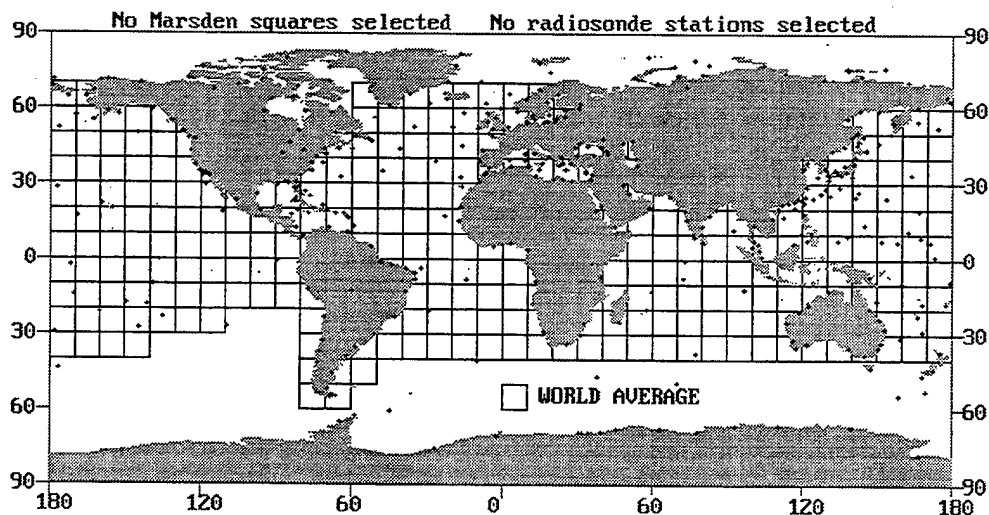


Figure 1. Representation of Marsden Squares.

Figure 1 shows a global perspective of the selected region and the criteria for dividing the whole world in small 10-degree by 10-degree

squares. On the other hand, Figure 2 gives the reader a better view of the area of interest, which goes from both the Venezuelan and Colombian coasts all the way up to Guantanamo Bay in Cuba.

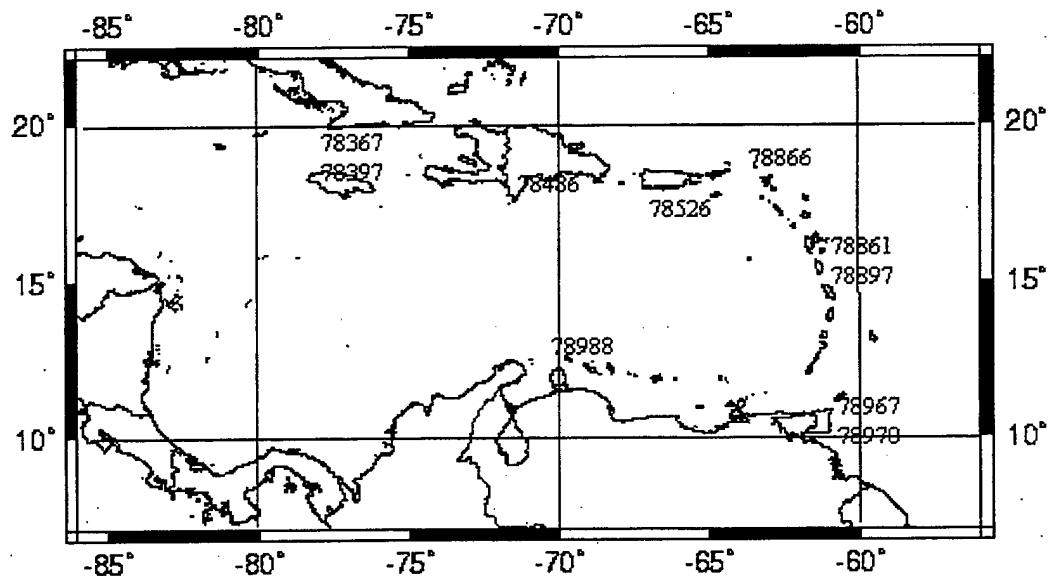


Figure 2. Stations in Marsden Squares 43 and 44.

B. CLIMATOLOGY

The Caribbean Sea presents two tropical periods: a dry or windy period from November to March and a humid or rainy period from July to September. In addition, two transition periods can be considered in between these tropical "seasons" [Ref. 2].

Because the sun is overhead in the Northern Hemisphere in July and overhead in the Southern Hemisphere in January, the zone of maximum heating shifts seasonally, so major pressure systems like the Intertropical Convergence Zone (ITCZ) shifts toward the north in July and toward the south in January [Ref. 3]. This ITCZ separates the northeast trade winds of the North Hemisphere from the southeast trade winds of the South Hemisphere, and strongly influences the climate of the area.

In summer, the subtropical high moves toward the pole and the ITCZ invades this area, producing abundant rainfall. On the other hand, the subtropical high moves toward the equator producing clear dry weather in winter [Ref. 4].

Local phenomena, such as sea-breezes and land-sea winds, which are caused by different heating rates of land and water during the day, are known to cause strong inversion layers in coastal areas. The breezes are frequent and strong enough to dominate the general circulation [Ref. 4]. These can affect propagation and therefore the local circulation for the region should be taken into account in order to completely model the environment.

C. ATMOSPHERIC CONDITIONS

The method used to determine atmospheric conditions and propagation phenomena was the program SDS from the EREPS suite. The program SDS displays an annual climatological surface summary for selected Marsden Squares. The statistics displayed within SDS are derived from two meteorological databases: the Radiosonde Data Analysis II assembled by the GTE Sylvania Corporation and the Duct 63 assembled by the National Climatic Data Center. GTE Sylvania Analysis is based on approximately three million radiosonde soundings taken during a five-year period, from 1966 to 1969 and 1973 to 1974. On the other hand, Duct 63 analysis is a fifteen-year subset of over 150 years of worldwide surface meteorological observations obtained from ship logs, ship weather reporting forms, published observations, automatic buoys, etc.

There are ten radiosonde stations located in the Marsden Squares 43 and 44. Although radiosonde stations in the same Marsden Square are completely independent, meteorologically speaking, in this study those radiosonde stations which are located very close, could be averaged. Figures 3 and 4 summarize the World Meteorology Organization Identification (WMO ID), Latitude, Longitude, Name and

Radiosonde Station in Marsden Squares 43 and 44. Considering both proximity between stations and similarities between outputs given by SDS, the area was divided in the following five zones:

1. Curacao Zone.
2. Trinidad and Tobago Zone.
3. Antigua Zone.
4. Jamaica Zone.
5. Puerto Rico Zone.

RADIOSONDE STATIONS IN MARSDEN SQUARE: 43				
	WMO ID	LAT	LON	RADIOSONDE STATION NAME
<input checked="" type="checkbox"/>	78866	18.05 N	63.12 W	JULIANA AIRPORT, ST. MARTIN
<input type="checkbox"/>	78526	18.43 N	66.00 W	SAN JUAN/INT., PUERTO RICO
<input type="checkbox"/>	78897	16.27 N	61.52 W	RAIZET, GUADELOUPE, LA GUADELOUPE
<input type="checkbox"/>	78861	17.12 N	61.78 W	COOLIDGE FIELD, ANTIGUA, BRITISH ISLANDS
<input type="checkbox"/>	78988	12.20 N	68.97 W	DR. A. PLESMAN AIRPORT, CURACAO
<input type="checkbox"/>	78967	10.70 N	61.60 W	CHAGUARAMAS, TRINIDAD
<input type="checkbox"/>	78970	10.62 N	61.35 W	PIARCO/PORT OF SPAIN, TRINIDAD + TOBAGO
<input type="checkbox"/>	78486	18.47 N	69.88 W	SANTO DOMINGO, DOMINICAN REPUBLIC

Figure 3. Radiosonde Stations in MS 43.

RADIOSONDE STATIONS IN MARSDEN SQUARE: 44				
	WMO ID	LAT	LON	RADIOSONDE STATION NAME
<input checked="" type="checkbox"/>	78397	18.07 N	76.85 W	KINGSTON/PALISADOES, JAMAICA
<input type="checkbox"/>	78367	19.90 N	75.15 W	GUANTANAMO, ORIENTE, CUBA

Figure 4. Radiosonde Stations in MS 44.

Table 1 shows some features given by SDS. These features are Average Elevated Duct Height (AEDH), Average Wind Speed (AWS), Surface Based Duct Occurrence (SBDO), Average Surface Based Height (SBDH), Effective Earth Radius Factor (K), Thickness (THIC), Average Surface N-unit Value (ANSB), and Number of stations averaged in each zone (NSZ). Data referenced in Table 1 is used as input for other EREPS programs, such as COVER and PROPR, to calculate radar coverage and propagation loss.

Features	Curacao	Trinidad	Antigua	Jamaica	Puerto Rico
AEDH (m)	17.6	17.6	17.6	17.6	17.6
AWS(kts)	13.4	13.4	13.4	14.6	13.4
SBDO(%)	3.0	12.5	6.0	19.0	10.0
SBDH(m)	88.0	120.0	110.5	121.5	125.7
K	1.653	1.602	1.610	1.602	1.608
NSZ	1	2	2	3	3
THIC(m)	88	120	110	122	126
ANSB	379	376	376	371	373

Table 1. Atmospheric condition in the selected zones.

Important information about the atmospheric condition of the Caribbean Sea region can be extracted from Table 1. It is very likely to have similar values of evaporation ducts, wind speed, and surface N-value. On the other hand, there is a great difference between Surface Based Ducts Occurrence; it changes from 3% in the Curacao zone to 19% in Jamaica.

III. EFFECTS OF THE ATMOSPHERE ON EM WAVES PROPAGATION

A. EM WAVE PROPAGATION

At radar frequencies, EM waves propagate from point-to-point via four different components: ground wave propagation, sky wave propagation, scatter propagation, and space wave propagation.

Ground wave propagation consists of a surface wave, which follows the contour of the earth. EM waves from ELF to mid MF propagate via this mechanism. At ELF it can be compared with a waveguide bounded by the earth and the ionosphere [Ref. 1]. At higher frequencies the wave is guided by the interface between the air and the earth's surface. In addition, daily and seasonal changes do not affect the ground wave propagation, so it is stable.

Sky wave propagation occurs when the ionosphere refracts the wave back to earth. Sky wave propagation affects the upper mid MF and HF. Likewise, it is associated with the various ionospheric layers, designated D, E, and F. These layers are not uniform and are subject to solar disturbances, so it changes with the time of the day [Ref. 1].

Scattered wave propagation is the result of the EM waves scattering from a very large number of index-of-refraction

inhomogeneities in the atmosphere. Reflection may be produced in either the troposphere or the ionosphere. The first, also known as tropospheric scatter propagation, is the most common form. Likewise, by using these types of propagation, the line-of-sight range may be extended beyond the horizon. Tropospheric scatter propagation communication systems are used to link over the horizon distances of up to 700 km [Ref. 4].

Space wave propagation occurs in the VHF, UHF, and SHF bands. These bands include TV, FM radio, microwave, and radar, which is the subject that this thesis focuses on. Space wave propagation occurs in the troposphere due to varying properties of the air, but not by the ionosphere which is the case for ground and sky wave propagation. However, pressure, temperature, and humidity of the troposphere dramatically affect the wave speed and these changes with respect to the altitude determine the degree of refraction of the space wave [Ref. 1].

B. ATMOSPHERIC INFLUENCE AND INDEX OF REFRACTION

Vertical gradients in atmospheric pressure (P), temperature (T), and water vapor (e) affect propagation in frequency ranges above VHF.

Likewise, the effects of these gradients are dominant in the troposphere.

This is due to the index of refraction (n), which is defined by

$$n \cong 1 + \rho \frac{2\pi A}{M} \left[\alpha + \frac{1\mu^2}{3KT} \frac{1}{(1 + j\omega\tau)} \right] \quad (1)$$

where:

ρ = Density of the air

A = Avogadro's number

M = Molecular weight

K = Boltzman's constant

μ = Permanent electric dipole moment

α = Polarizability coefficient

τ = Relaxation of time for external field

ω = Angular frequency of external field

This equation shows the Debye index of refraction representation for gases after some additional assumptions [Ref. 4]. Two important features can be extracted from it: first, n is frequency dependent, and second, all type of gases present in the atmosphere affect the first term, polarization, of the equation.

Due to the fact that for VHF/UHF/Microwave frequency bands the term $\omega\tau \ll 1$, the frequency dependency condition can be neglected. On the other hand, only water vapor contributes to the second term (dipole moment) of the equation.

The index of refraction is very close to 1 for VHF/UHF/Microwave frequency bands so term refractivity (N) is introduced

$$N = (n - 1) \times 10^6 \quad (2)$$

For frequencies between 100 MHz and 80 GHz, the following equation can be applied when atmospheric values of P , T , and e are known:

$$N = 77.6 \frac{P}{T} - 5.6 \frac{e}{T} + 3.73 \times 10^5 \frac{e}{T^2} \quad (3)$$

Finally, when ducts are present, the refractivity index can be converted to new units. This modified refractive index (M) adds 157 N -units per kilometer to all N -values. The importance of the modified refractivity index is that for a duct to exist, the M -gradient must be negative somewhere in the profile.

C. STANDARD AND REFRACTIVE GRADIENTS

The model most suitable for propagation studies is the standard atmospheric model, in which the index of refraction increases linearly with height. This increment of the refraction index causes the EM ray to

bend downward. The effect is accounted for by increasing the effective radius of the earth by a factor of $4/3$ and then assuming that there is no ray curvature for propagation over this larger earth [Ref. 6].

The standard atmospheric model cannot be always applied, due to the fact that the atmosphere has variable conditions, in which an increase of the refractive index occurs with altitude instead of a reduction of it with altitude.

EREPS gives a classification for refractive conditions by placing distinctive values for N and M gradients. These conditions can be subrefractive, normal, superrefractive, or trapped depending on characteristic values of N and M .

Subrefraction occurs when the temperature and humidity distribution creates an increasing value of N with altitude and the ray is bent upward, and propagates away from the earth.

The refractive distribution is assumed to decrease almost linearly with height. This is known as a normal or standard condition, which is characterized by a decrease of 39 N-units per kilometer or 118 M-units per kilometer. Indeed, standard gradients produce a bending in the EM ray downward from the straight line.

Superrefraction occurs when the atmosphere's temperature increases and/or the water vapor content decreases rapidly with height,

making the ray bend downward until the critical gradient is reached. The point where the earth radius and the radius of curvature of the ray are equal is called the critical gradient.

It is said that there is a trapping condition when the ray is bent so that it either strikes the earth surface or enters a standard refraction region. When it enters a standard refraction region, it can be refracted back upward and reenter the area of refractivity gradient that first caused the downward refraction.

Table 2 [Ref. 1] summarizes the gradient values associated with the refractive conditions (N-gradient, M-gradient) and their relationship with range discussed above.

Classification	N-gradient (N/Km)	M-gradient (M/Km)	Distance to surface horizon
Subrefraction	> 0	> 157	Reduced
Normal	- 79 to 0	79 to 157	Normal
Superrefraction	-157 to -79	0 to 79	Increased
Trapping	< -157	< 0	Greatly Increased

Table 2. EREPS Refractive Gradients and Distance relationship.

D. TRAPPING LAYERS AND DUCTS

There are differences between trapping layers and ducts. Trapping layers are produced in a region where the M -gradient is less than zero (same as N -gradient < -157 N/Km). In this case, the ray is bent toward the earth's surface. When a trapping layer does not extend down to the surface it is called an "elevated layer." On the other hand, a duct is the region associated with the trapping layer; in a duct the EM energy is confined and channeled between its top and bottom. The top of the duct is always the top of the trapping layer. However, the bottom of the duct can extend below the bottom of the trapping layer. In addition, ducts which have their lower boundary at the surface are called "surface based ducts," and ducts which have their lower boundary above the surface are called "elevated ducts" [Ref. 4].

Finally, there is another kind of duct called an "evaporation duct," which is produced by an abrupt change in relative humidity at the water-air interface (from 100% to 80% in the first few meters). Evaporation ducts are almost always present over water, so their effects are important in most modern naval operations. Evaporation duct thickness varies with changes in temperature and wind velocity at the surface during the day.

Likewise, the thickness of the evaporation duct is related to the minimum frequency that can be propagated within the duct [Ref. 7].

Figure 5 graphically summarizes the different classifications of ducts and their relationship to the altitude and M -value.

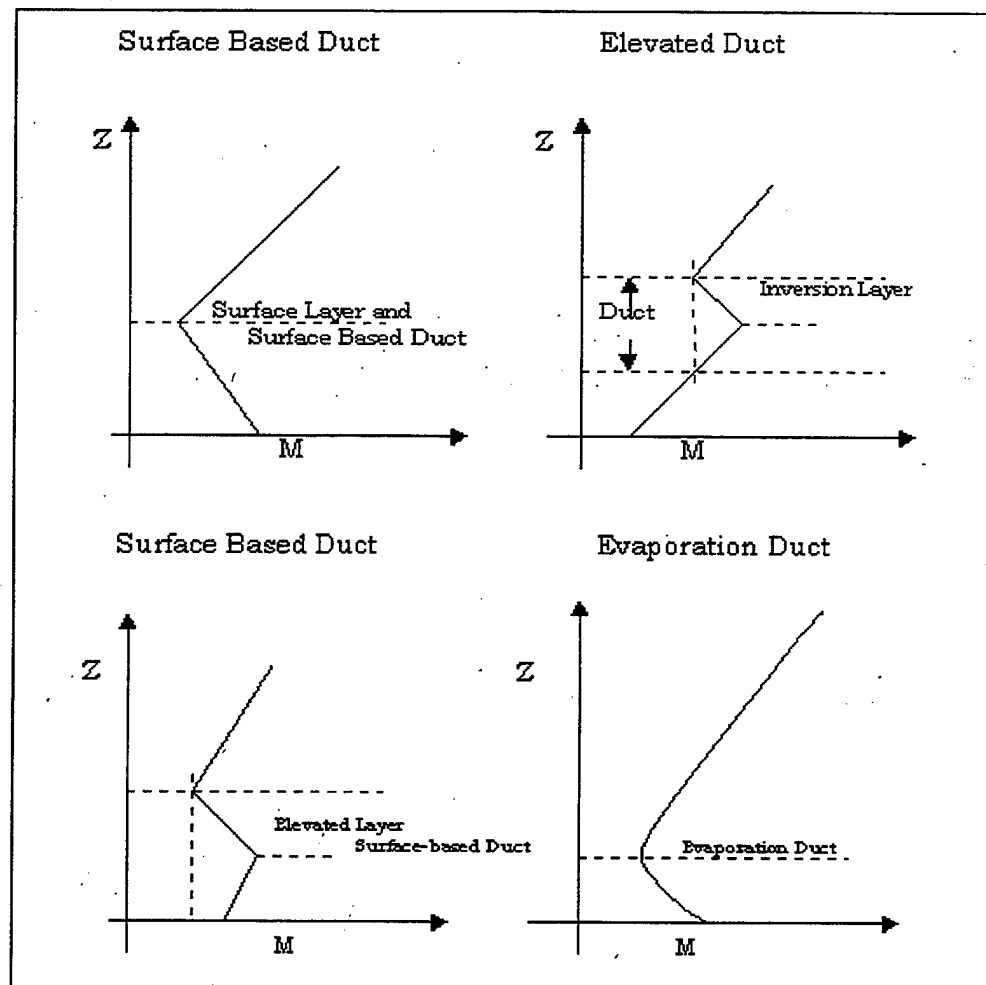


Figure 5. Refractive Profiles of ducting.

IV. RADAR SYSTEMS

The use of radar systems in the military include detection and location of aircraft, of moving targets in the battlefield, of ships, and intruder alarms, among others. Radar systems can be static or they can operate mounted on different platforms, such as vehicles, aircraft, and ships. This chapter focuses on selected radar systems; land based and ship mounted radars are used in this study. Those radars are not only in use by the different armed forces from countries in the region, such as Colombia, USA, and Venezuela, but also are produced by different manufactures in different countries.

Selected radar systems from the region have different nominal ranges. For example, both the TPS-70 and SPS-49 radars, which have a nominal range of more than 400 kilometers, can be considered as long-range air search radars. On the other hand, radars such as Sea Tiger, RAN-10S, Giraffe, and Falcon, with nominal ranges between 75 and 150 kilometers, can be classified as medium-range air surveillance radars. Finally, there are other radar systems used to track (with nominal ranges up to 50 kilometers), or for short-range air defense, that are not considered in this study.

The reason for selecting radar systems with different ranges is so that there are three basic types of Air Defense Systems depending upon proximity to a valuable resource. These basic types are Warning, Area, and Point [Ref. 8]. Table 3 summaries the basic types of defense systems, weapons associated to each defense system, and sensor types used.

Defense System	Weapon	Sensor Type
Warning	Area/Point Defense	Early Warning Radar
Area	Interceptor	GCI Radars
	Long Range SAM	Acquisition or Tracking Radars
Point	Med./Short Range SAM	Acquisition or Tracking Radars
	AAA	Optical /Video Radars

Table 3. Basic type of Air Defense Systems.

Some of the EREPS programs require an input value for Radar Cross Section (RCS), which is used to determine the effects of the environment upon the radar system, or relative performance between systems. RCS is a measure of the radar reflection characteristics of the target, and is equal to the power reflected back to the radar divided by power density of the wave striking the target [Ref. 9].

Many changes occur in the RCS of an aircraft when it is flying due to slight changes in viewing aspects. It is very difficult to completely and

concisely specify the RCS of a target [Ref. 10]. It is common to use a RCS of 1 square meter as a reference. However, in this study, a target with a RCS of 2 square meters was used as input data to the EREPS programs. This RCS value is equivalent to the size of a small fighter [Ref. 10].

The radar horizon is beyond the optical horizon due to the $4/3$ earth radius ratio. In many long-range missions aircraft and some types of missiles usually fly at low altitude to avoid being detected by radars [Ref. 11]. This altitude, which in many cases is below 1000 feet, may result in less than 100 km of detection distance when considering the optical horizon against a 40-meter high antenna. This common geometrical arrangement between the radar and missile may lead to incorrect simulation results in some cases [Ref. 10], so it is important to use accurate models of atmospheric refraction.

Table 4 shows the selected radar systems for this study and classifies them based on platform type.

Platform Type	Radar System		
Land-based	TPS-70	Falcon	Giraffe
Ship-mounted	SPS-49	RAN-10S	Sea Tiger

Table 4. Selected Radar Systems.

A. LAND-BASED RADAR SYSTEM

The TPS-70, Falcon, and Giraffe are land-based radars used for air defense systems. Data and specifications for each radar system are given in Table 5. It is important to notice that these data are estimates because the exact information about the systems is classified.

Table 5 summarizes specifications from selected land-based radar systems. Because manufacturer's specifications are usually classified, some estimates of the data and specifications were taken from Jane's Radar and EW Systems 98 [Ref. 12], and others were calculated. The estimates should be very close to the exact values.

Land-Based	TPS-70	Falcon	Giraffe
Frequency (GHz)	2.95	5	6.6
PRF (KHz.)	0.25	1.0	1.2
PW (μ sec)	6.5	2.0	1.66
Scan Rate (rpm)	6	12	30
Polarization	Linear	Horizontal	Linear
Antenna Type	Planar Array	High Gain	High Gain
Manufacturer	North-Grumm	ITT Gilfillan	Ericsson
Use	Air Surveillance	Air Surveillance	Search/Track
Power Output	3.5 MW	1.5 MW	200 KW
Range	440 Km	160 Km	75 Km
Antenna Height	15 m	15 m	15 m
Country	USA	USA	Sweden

Table 5. Specifications for selected land-based Radar Systems.

1. TPS-70

The AN/TPS-70 is a mobile E/F band radar designed to detect and track hostile aircraft in a variety of environments at ranges up to 450 kilometers. Manufactured in the United States by the Northrop Grumman Corporation, it incorporates clutter rejection and ECM features, with a low-sidelobe antenna. This radar also incorporates advanced signal analysis and processing techniques and a digital coherent moving target indicator system. The AN/TPS-70 is currently in production, and it is in operation in over 15 countries including the US for the Caribbean Basin Radar Network [Ref. 12].

2. Falcon

This G-band (4 to 6 GHz) radar is a two dimensional air/sea surveillance radar providing search, acquisition, and tracking of low-altitude aircraft and the simultaneous coastal surveillance and tracking of ships, small boats, and low-flying helicopters. Fabricated in the United States by the ITT Gilfillan company, this radar can transmit data in digital format to air and surface control centers at distant locations to provide centralized command and control operations.

The radar equipment can be installed in a protected bunker configuration, a shelter, or a mobile configuration, and it is designed for

unattended operation [Ref. 12]. Some countries in the Caribbean Basin use this radar system.

3. Giraffe

Giraffe is a family of combined G/H search radars and combat control centers for mobile and static short- or medium-range Command, Control, Communication and Intelligence air defense systems. This radar system manufactured in Sweden by Ericsson and has been designed to detect very low-flying targets in severe clutter and ECM environment.

Giraffe 75, which is operated by the Venezuelan Army, has a nominal detection range of 75 kilometers. In addition, it has automatic hovering helicopter detection, threat evaluation functions, and an antenna operating at a height of 13 meters, which extends the horizon by 5 to 10 kilometers compared with an antenna operating at 3 meters. Also it has altitude coverage from the ground to 10 kilometers [Ref. 12].

B. SHIP-MOUNTED RADAR SYSTEMS

In this study three ship-mounted radar systems were selected: SPS-49, Sea Tiger, and RAN-10S. These radars are on board Spruance class destroyers, Almirante Padilla class corvettes, and Lupo class

class destroyers, Almirante Padilla class corvettes, and Lupo class frigates respectively. Detailed information about these radars is given in Table 6.

Ship Mounted	Sea Tiger	RAN-10S	SPS-49
Frequency (GHz)	3.0	3.5	0.9
PRF (KHz.)	1.2	1.2	0.3
PW (μ sec)	1.8	1.6	6
Scan Rate (rpm)	30	30	12
Polarization	Linear	Linear	Circular
Antenna Type	Planar Array	High Gain	Cosec
Manufacturer	Thompson-CFS	Alenia	Raytheon
Use	Air Surveillance	Air Surveillance	Air Surveillance
Power Output	250 KW	240 KW	350 KW
Range	120 Km	150 Km	460 Km
Antenna Height	30 m	30 m	40 m
Country	France	Italy	USA

Table 6. Specifications for selected ship-mounted radar systems.

1. SPS-49

This UHF (300 to 1000 MHz) long-range air surveillance radar, built in the USA by Raytheon Company, was designed for use as the primary detection radar aboard various combatant ships of several countries.

AN/SPS-49 (V) 5 has the following features: high average power for long-range surveillance and detection of low RCS targets, horizon stabilized antenna for consistent elevation coverage, automatic target detection and rapid designation of all target threats, and high ECM for assured surveillance in a hostile environment [Ref. 12].

2. RAN-10S

RAN-10S is a F-band (3 to 4 GHz.) air and surface surveillance radar manufactured in Italy by Alenia Elsig Sistemi Navali. It is on board of the Lupo class frigates from the Venezuelan Navy. It is suitable for installation on medium tonnage ships, such as destroyers, frigates and corvettes. The main features are high elevation coverage, high data rates and high precision/resolution. Also, it uses a coded waveform in conjunction with digital processing of received signals [Ref. 12].

Typical operational roles include air warning against aircraft and missiles, direction of both fixed- and rotary-wing aircraft, surface surveillance, navigation and direction of surface-to-surface missiles.

3. Sea Tiger

The French E/F-band (2 to 4 GHz) air and surface surveillance and target designator radar was developed by Thomson-CSF, and is on board of the Almirante Padilla class corvettes from the Colombian Navy.

Sea Tiger was designed to provide detection and tracking of missiles, including sea-skimming anti-ship weapons. It can be used to perform several functions in a very severe clutter and jamming environment, such as air surveillance, surface surveillance, anti-missile surveillance and target designation [Ref. 12].

V. DATA ANALYSIS AND RESULTS

Climatological data from each radiosonde station, analysis procedures, and future enhancements for atmospheric data collection are described in this chapter. Ten (10) radiosonde stations were selected from Marsden Squares 43 and 44. The number of radiosonde stations in the area, proximity between stations, and the similarity of the output values allowed for the division of two the Marsden Squares into five zones in order to facilitate the analysis.

Annual climatological surface duct summary from each station was extracted using SDS. Data were analyzed, and then used as input to COVER to investigate both the effects of the environment upon systems performance, and the relative performance between selected radars. Also, some data were used in PROPR to calculate and display the propagation loss in decibels versus range graphically. SDS gives important data that can be used as input for other programs from the suite. These data are:

- Percent occurrence histogram of evaporation duct heights.
- Evaporation duct height.
- Surface wind speed.
- Number of observations.
- Percent occurrence of surface-based ducts.
- Surface-based duct height.

- Surface-based duct occurrence.
- Surface N -unit value.
- Effective earth radius factor (K).

Evaporation duct height (EDH), surface wind speed (AWS), surface-based duct height (SDH), surface N -unit value (NSUBS), and effective earth radius factor (K) are used as input for COVER and PROPR. Percent of occurrence is an important parameter, which is addressed in following chapters.

It is important to note that it has been assumed that the radars are located at places (or on board of ships) close enough to stations where data are collected, in order to assure conditions remain unchanged, or horizontal homogeneity inside each zone.

In practice, data from radiosonde stations and ships are frequently taken far away from places where military operations are executed. This may cause some errors because the atmosphere is not horizontally homogeneous. It is important to obtain data close to places where operations are to be carried out, in order to avoid errors. A tool for the enhancement of atmospheric data collection from the battlefield is the Tactical Dropsonde (TDROP), which is an expendable electronic payload that acquires atmospheric environmental data, and transmits it via a real time RF data link compatible with tactical aircraft receivers [Ref. 13].

A. DATA ANALYSIS FOR LAND-BASED RADARS

Propagation effects for land-based radars were analyzed in the Curacao, and Trinidad and Tobago zones because countries like Venezuela and Colombia operate the selected systems. Specifications for selected land-based radars appeared in Table 5.

On the other hand, propagation effects for ship-based radars were analyzed in the Antigua, Puerto Rico, and Jamaica zones. Indeed, data from ship-based radars belonging to the Colombian, the Venezuelan, and the United States navies were selected, and their specifications were summarized in Table 6.

1. Curacao Zone

The Curacao zone has only the Dr. A. Plesman Airport radiosonde station (WMOID 78988) in Curacao. Figure 6 shows the climatological data from Curacao.

This part of the study is characterized by the use of COVER with data from SDS, and selected land-based radars. COVER gave the output

shown in Figures 7, 8, and 9. The figures correspond to the TPS-70, Falcon, and Giraffe radars respectively.

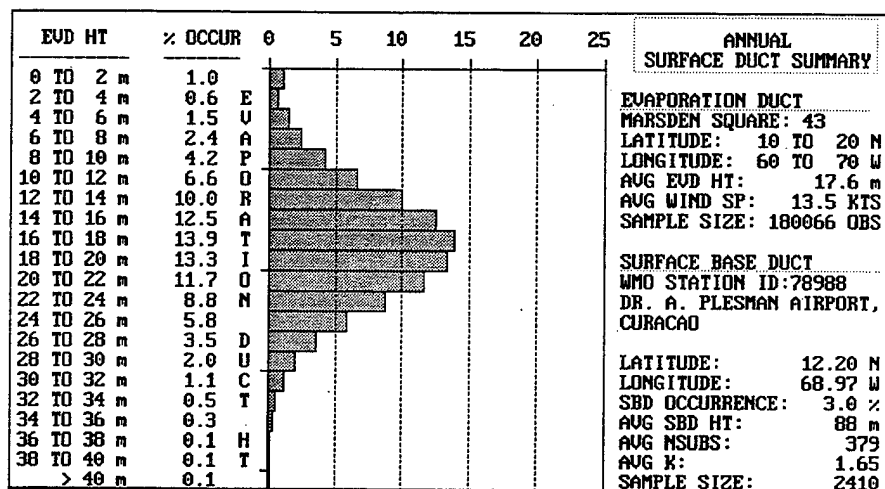


Figure 6. Evaporation Duct Summary, Curacao zone.

A visual inspection of Figure 7 shows that the Optimal Altitude to Avoid Detection (OAAD) by the TPS-70 radar with Curacao conditions, is approximately 770 feet with a Detection Distance (DD) of 109.4 kilometers when there are ducting conditions, and 92 km when there are no ducts. For the case of a flying target with a RCS of 2 square meters (at 1000 feet above ground) should be detected at 115 km when ducting conditions are present, and at 95 km if there are no ducts. This detection distance difference of 20 km is important for a tactical aircraft, which usually flies at 500 kts, because this distance may represent a gate of more than 1 minute of flying time.

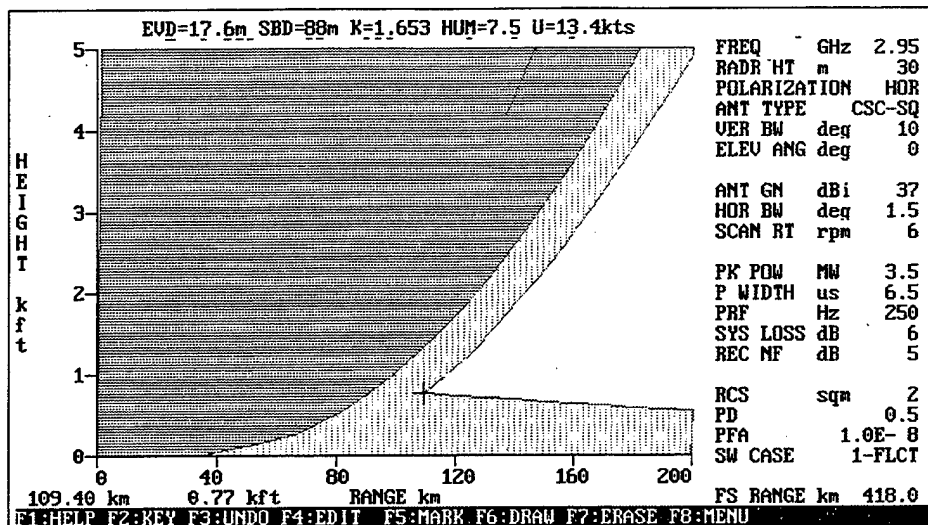


Figure 7. COVER output for TPS-70 radar, Curacao zone.

Figure 8 represents the COVER output for a Falcon radar in Curacao. The same figure shows an OAAD of 650 feet, and a DD of 97.4 km for ducting conditions, and a DD of 82.5 km for no ducting. Likewise, an aircraft at 1000 feet should be detected at 87 km in an environment with no ducts, and at 108 km with ducts. This results in a DD difference of 21 km.

Figure 9 corresponds to the COVER output for Giraffe radar in Curacao. Here an OAAD of 450 feet, 70.8 kilometers can be observed for ducting conditions, and a DD of 64 km for no ducting. The figure also shows that an aircraft at 1000 feet should be detected at 81 km in an environment with no ducts, and at 94 km with ducts. This results in a DD difference of 13 km.

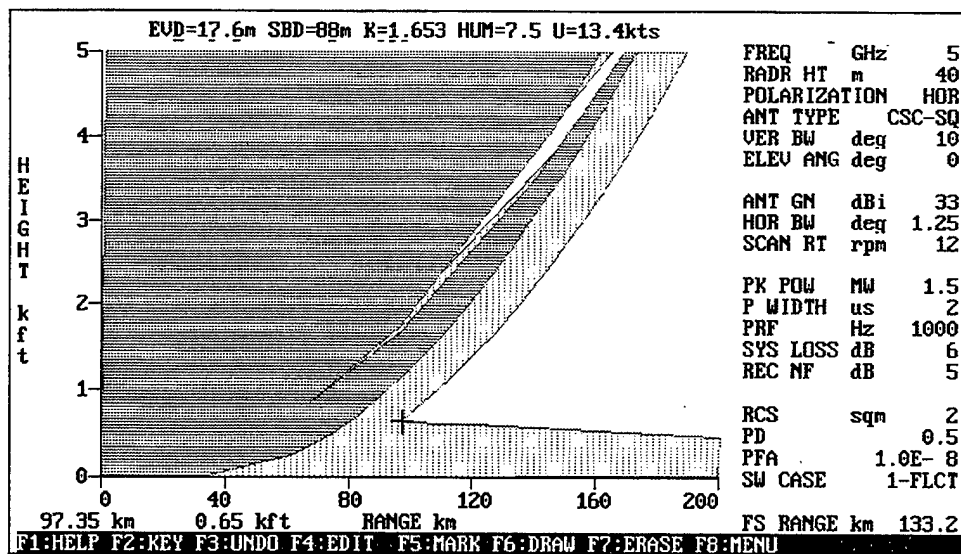


Figure 8. COVER output for Falcon radar, Curacao zone.

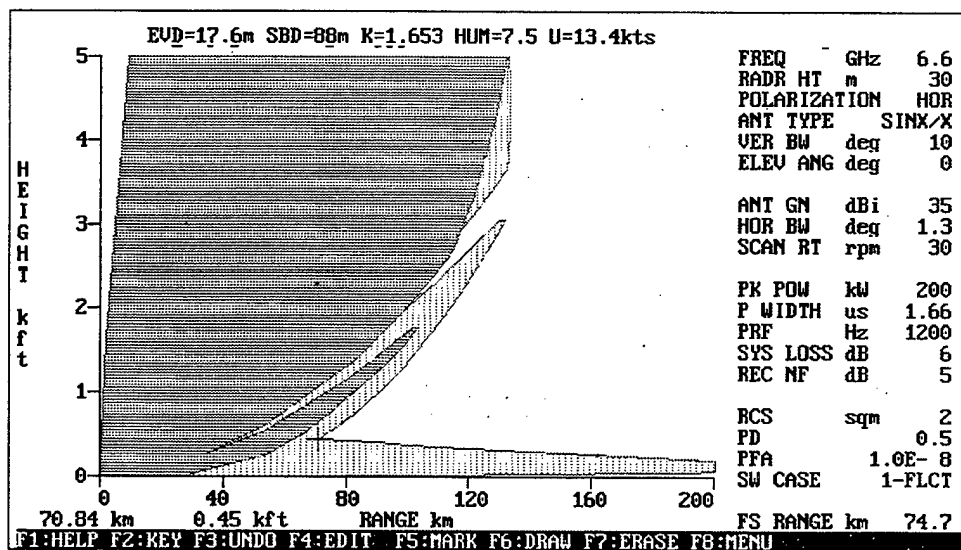


Figure 9. COVER output for Giraffe radar, Curacao zone.

Data given by SDS were also used as input for PROPR to calculate propagation loss. Figure 10 represents the PROPR output for a TPS-70

radar with data from the selected area, and shows its ability to detect a target at OAAD. For this target, the resultant DD were 83 km without ducting and 103.6 km with ducting.

Although those detection distances from both COVER and PROPR are not exactly equal, the DD difference between ducting and no ducting conditions remains almost the same (see Table 7). Differences in the outputs are due to COVER's parallel ray approximation, as will be discussed later.

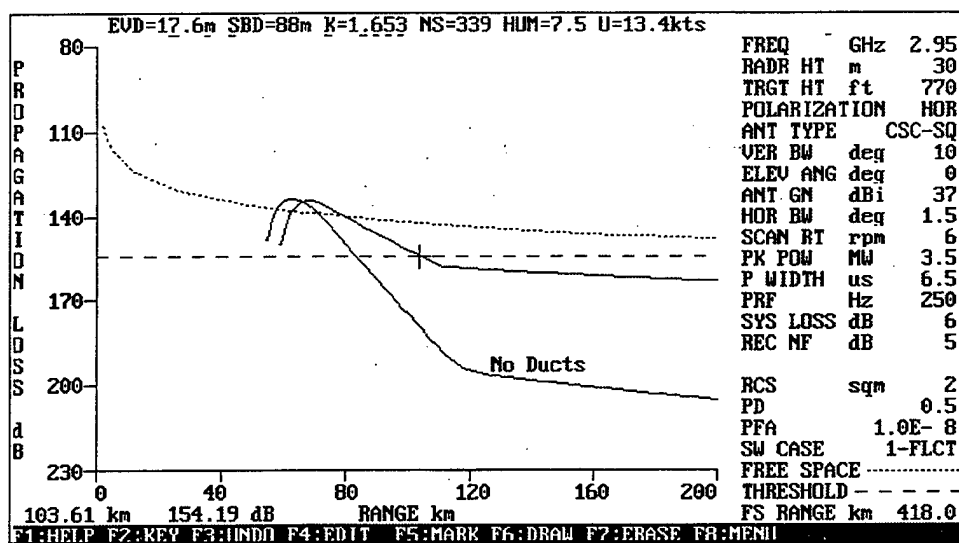


Figure 10. PROPR output for TPS-70 radar, Curacao zone.

Similar results are given by Figures 11 and 12. Those figures show the PROPR outputs for Falcon and Giraffe radar in the Curacao zone.

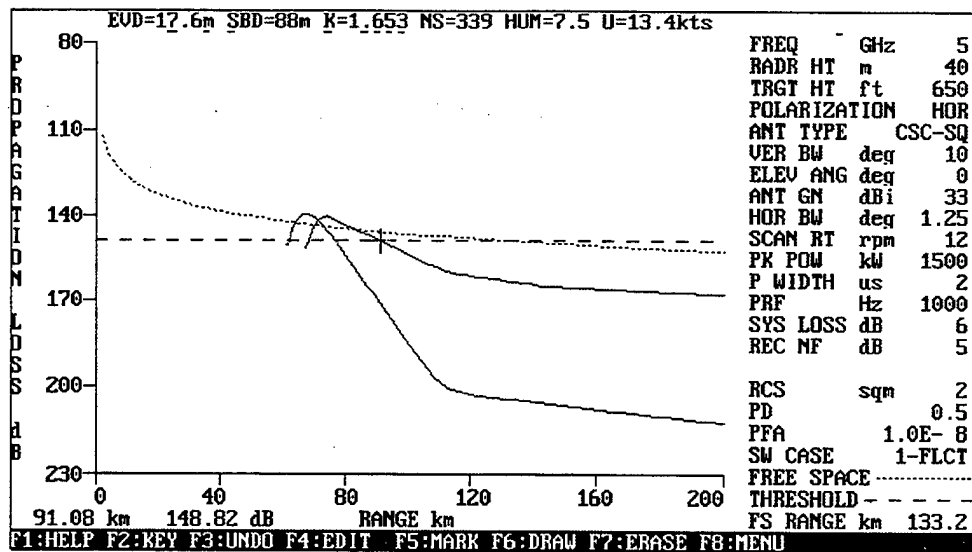


Figure 11. PROPR output for Falcon radar, Curacao zone.

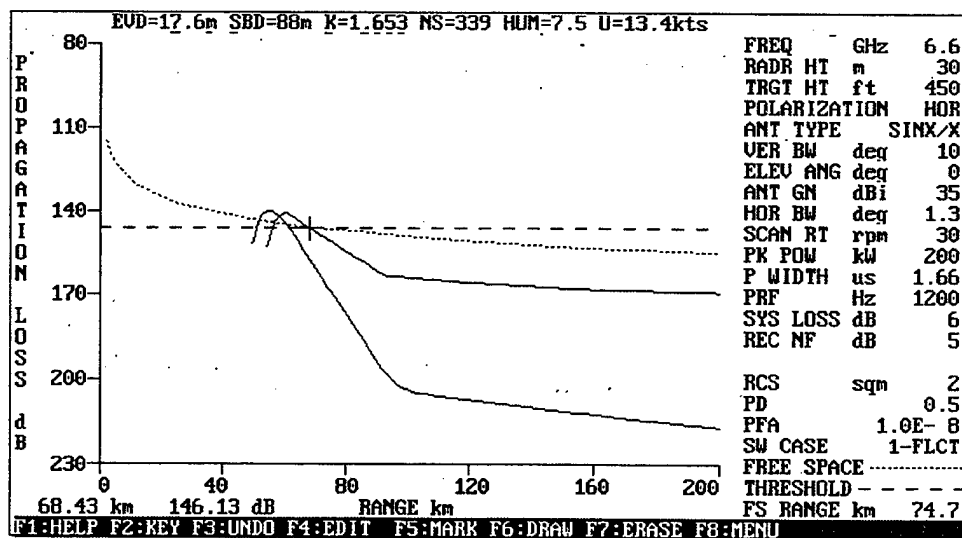


Figure 12. PROPR output for Giraffe radar, Curacao zone.

A DD of 76 km for no ducting conditions, and 91 km for ducting can be found in Figure 11 for the Falcon radar using PROPR. On the

other hand, a DD of 59.7 km for no ducting and 68.4 km for ducting conditions are given in Figure 12 for the Giraffe radar. Detection distance differences of 15 and almost 9 km result as illustrated in Figures 11 and 12. These detection distance differences are not the same values obtained from COVER outputs given in Figures 8 and 9.

Table 7 shows the Detection Distance difference between values given by COVER and PROPR when comparing land-based radars for conditions in the Curacao zone.

PROGRAMS	RADAR	DD no ducts	DD with ducts	DD Difference
COVER	TPS-70	92	109.4	17.4
	Falcon	97.4	82.5	14.9
	Giraffe	70.8	64.0	6.8
PROPR	TPS-70	83.0	103.6	20.6
	Falcon	91.1	77.0	14.1
	Giraffe	62.0	68.4	6.4

Table 7. Detection Distance Summary, Curacao zone.

2. Trinidad and Tobago Zone

The analysis of the Trinidad and Tobago zone consisted of using both COVER and PROPR with data from SDS, and the same land-based radars selected in Table 5. Figure 13 summarizes the climatological data for the Trinidad and Tobago zone.

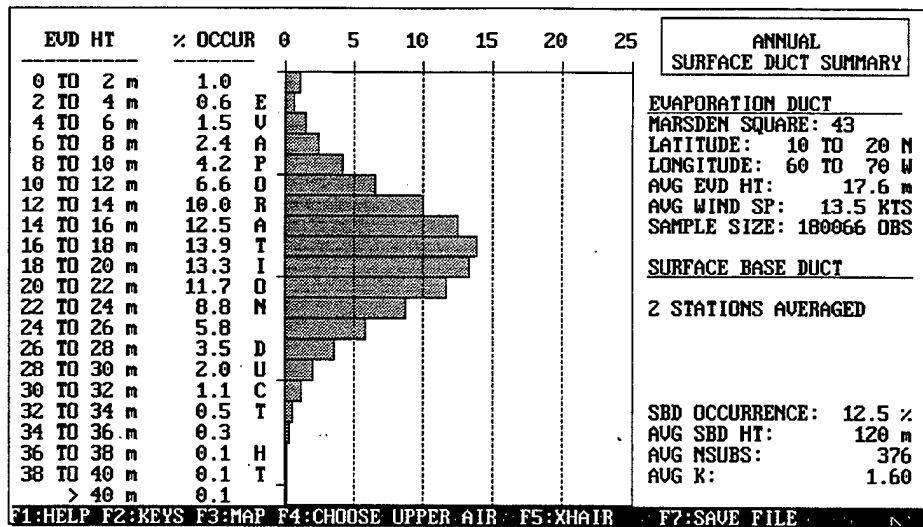


Figure 13. Evaporation Duct Summary, Trinidad zone.

COVER produced Figures 14, 15 and 16, which correspond to TPS-70, Falcon and Giraffe respectively.

Figure 14 shows an OAAD for the TPS-70 radar of 900 feet approximately, and a DD of 113.3 km, when there are ducting conditions, and 92 km for no ducts. If an aircraft is flying at an altitude of 1000 ft, the DD should be 116 km when ducting conditions are present, and 98 km if there are no ducts. This result in a DD difference of 18 km.

Figure 15 shows the COVER output for the Falcon radar based on the Trinidad and Tobago climatological soundings. Here, an OAAD of 650 feet, at 96.9 kilometers can be observed for ducting conditions and 82.5

km for no ducts. Also, an aircraft at 1000 feet should be detected at 92 km in an environment with no ducts, and at 110 km with ducts, which results in a DD difference of 18 km.

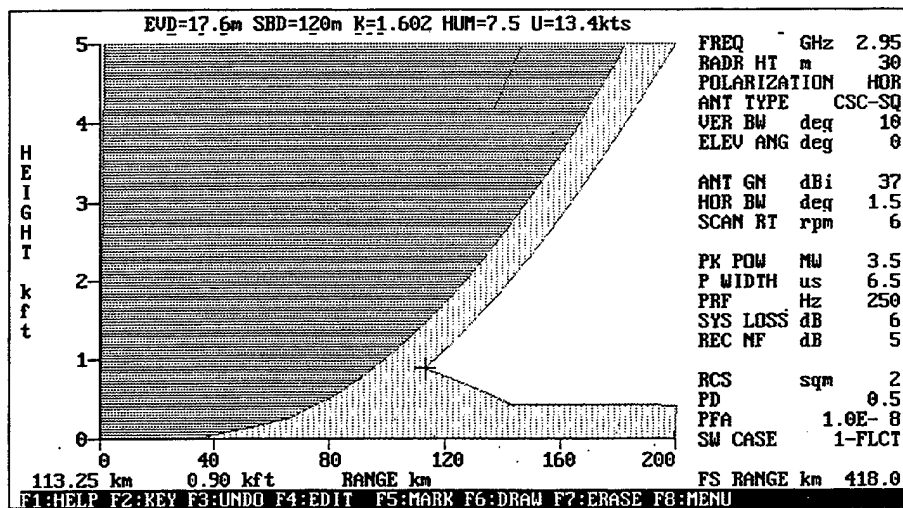


Figure 14. COVER output for TPS-70, Trinidad zone

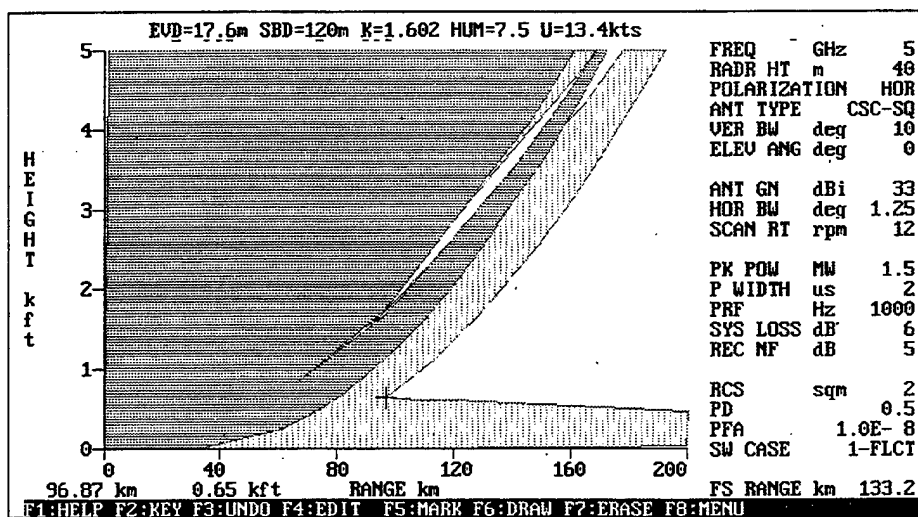


Figure 15. COVER output for Falcon radar, Trinidad zone.

Figure 16 corresponds to the COVER output for the Giraffe radar with Trinidad and Tobago conditions. Here an OAAD of 450 feet, at 70.8 km can be observed for ducting conditions, and 64 km for no ducts. For an aircraft at 1000 feet, the DD is 83 km in an environment with no ducts, and 94 km with ducts. This results in a detection distance difference of 11 km.

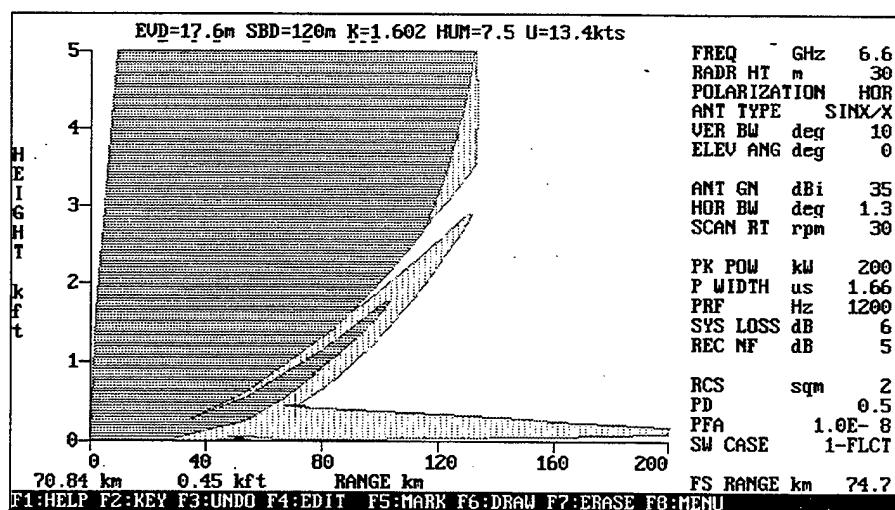


Figure 16. COVER output for Giraffe radar, Trinidad zone.

Figure 17 shows the PROPR output for a TPS-70 radar with the Trinidad and Tobago zone conditions. Also Figure 17 shows the radar's ability to detect a 2-meter square RCS target at OAAD. The DD without

duct conditions was 80.3 km, compared to 103 km with average ducting conditions.

Figure 18, which corresponds to PROPR output for a Falcon radar with the Trinidad zone conditions, gives a DD of 78 km when there are no ducts, and 89.6 km when ducts are present. In contrast, Figure 19, which represents PROPR output for Giraffe radars operating in the same zone, gives a DD of 60.7 km if there are no ducts, and 68.4 km for ducting conditions.

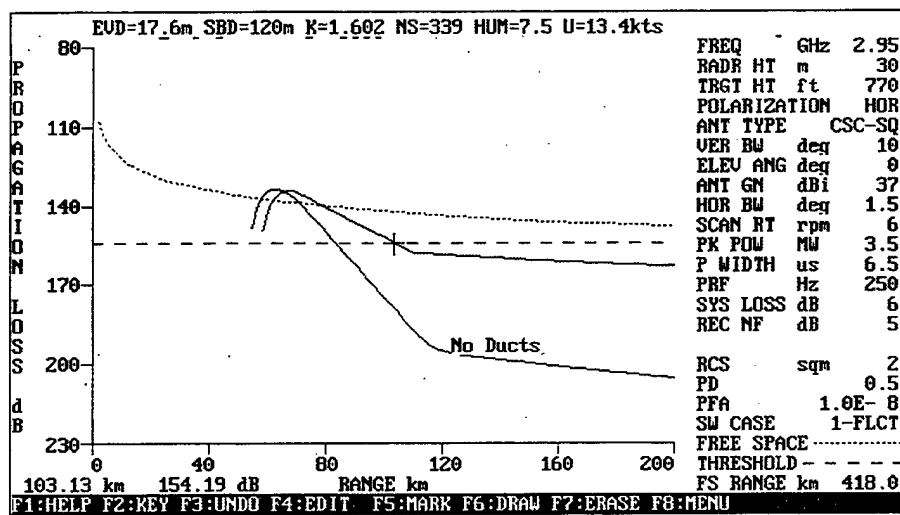


Figure 17. PROPR output for TPS-70 radar, Trinidad zone.

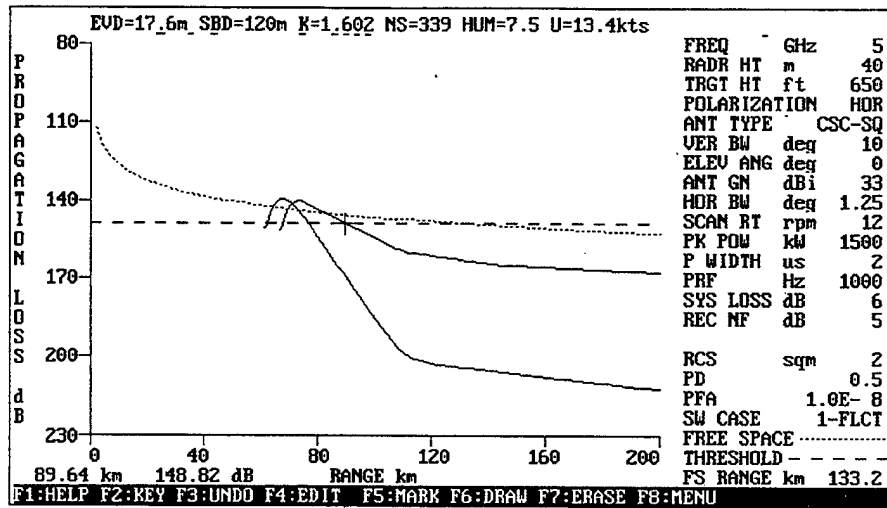


Figure 18. PROPR output for Falcon radar, Trinidad zone.

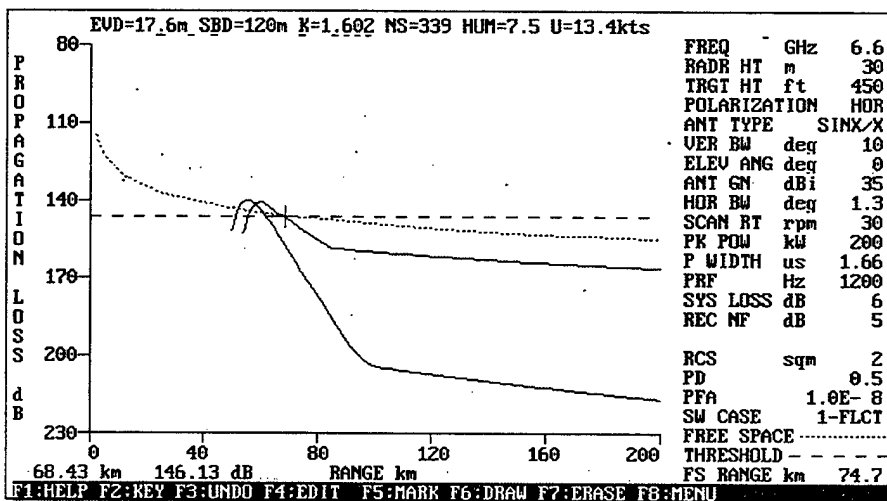


Figure 19. PROPR output for Giraffe radar, Trinidad zone.

When comparing outputs given by COVER and PROPR, it can be seen that the distances are very similar for a given radar system. However, slight differences are due to the fact that COVER uses a parallel ray approximation to the propagation model, and this

assumption may produce errors at low altitudes. In contrast with COVER, the PROPR program does not make the parallel ray approximation, so the results taken from PROPR are considered to be more accurate for all geometries [Ref. 1].

Table 8 shows the Detection Distance difference between values given by COVER and PROPR when comparing land-based radars and data for conditions in the Trinidad and Tobago zone.

PROGRAMS	RADAR	DD no ducts	DD with ducts	DD Difference
COVER	TPS-70	92	113.25	21.25
	Falcon	96.9	82.5	14.4
	Giraffe	70.8	64.0	6.8
PROPR	TPS-70	83.0	103.1	20.1
	Falcon	89.6	77.0	12.6
	Giraffe	62.0	68.4	6.4

Table 8. Detection Distance Summary, Trinidad zone.

B. DATA ANALYSIS FOR SHIP-MOUNTED RADARS

1. Antigua Zone

The Antigua zone data is based on two radiosonde stations. They are Raizet (WMOID 78897) located in La Guadeloupe, and Coolidge Field (WMOID 78861) located in Antigua, British Islands. This zone was

analyzed by using COVER with data from SDS, as given in Figure 20, and with specifications of selected ship-mounted radars as given in Table 6. COVER gave the output shown in Figure 21 for Sea Tiger, Figure 22 for RAN-10S, and Figure 23 for SPS-49.

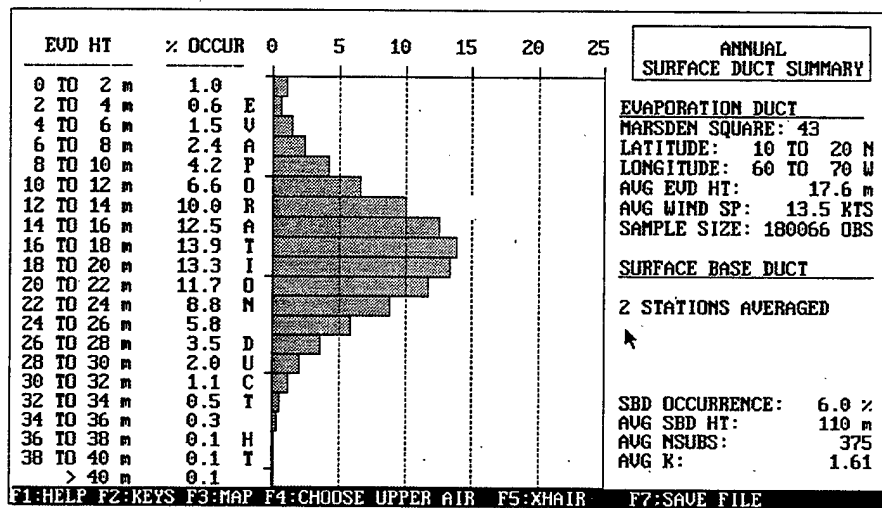


Figure 20. Evaporation Duct Summary, Antigua zone.

Figure 21 shows an OAAD for a Sea Tiger radar of 390 feet with a DD of 77.1 km for ducting conditions, and a DD of 63 for no ducts. If an aircraft is flying at an altitude of 1000 ft, the DD should be 102 km when ducting conditions are presented, and 84 km if there is no ducts. This is a DD difference of 18 km.

Figure 22 shows the COVER output for a RAN-10S radar with the Antigua zone duct conditions. Here, an OAAD of 380 feet, at 76.63 km

can be observed with ducting conditions, and a DD of 64 km with no ducts. Likewise, an aircraft at 1000 feet should be detected at 83 km in an environment with no ducts, and at 97 km with ducts, which results in a DD difference of 14 km.

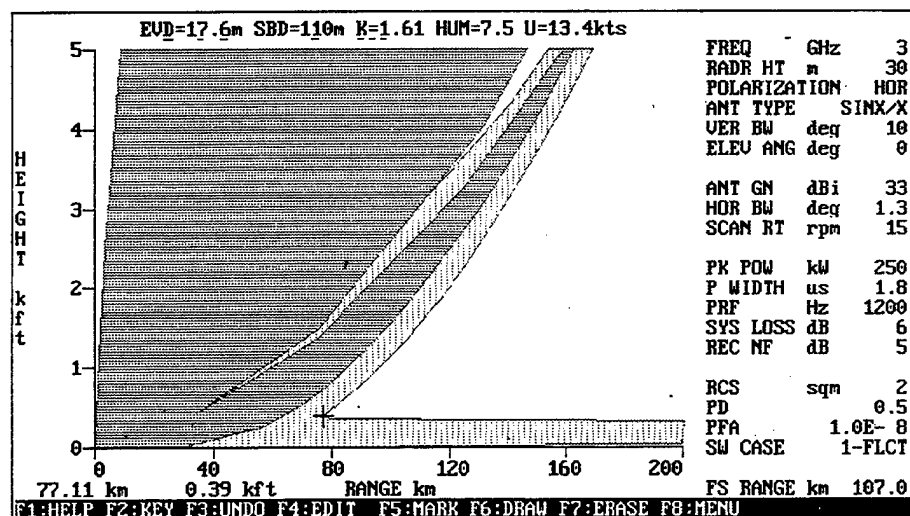


Figure 21. COVER output for Sea Tiger radar, Antigua zone.

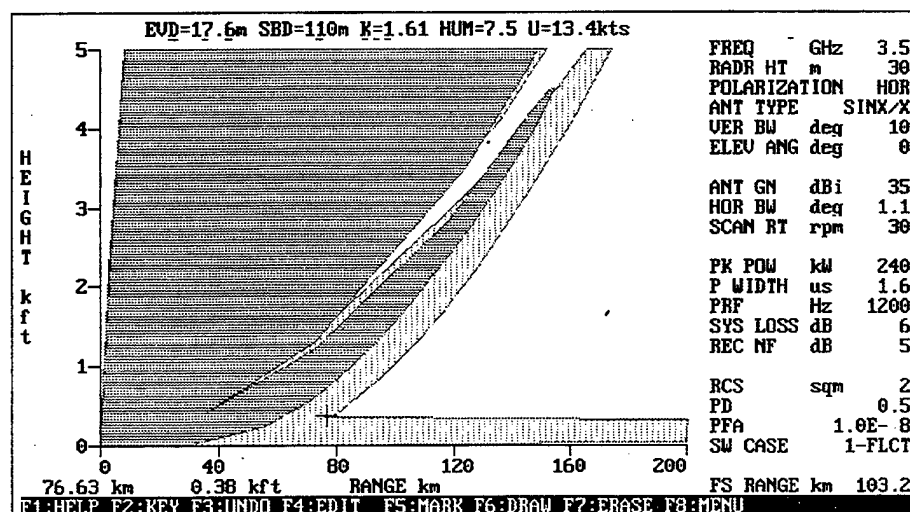


Figure 22. COVER output for RAN-10S, Antigua zone.

Figure 23 corresponds to the COVER output for the SPS-49 radar with the Antigua zone conditions. An OAAD of 860 feet, at 78.1 km can be observed with ducting conditions, and DD of 101 with no ducts. For an aircraft at 1000 feet, a DD of 91 km in an environment with ducts, and at 106 km without ducts, or a DD difference of 15 km.

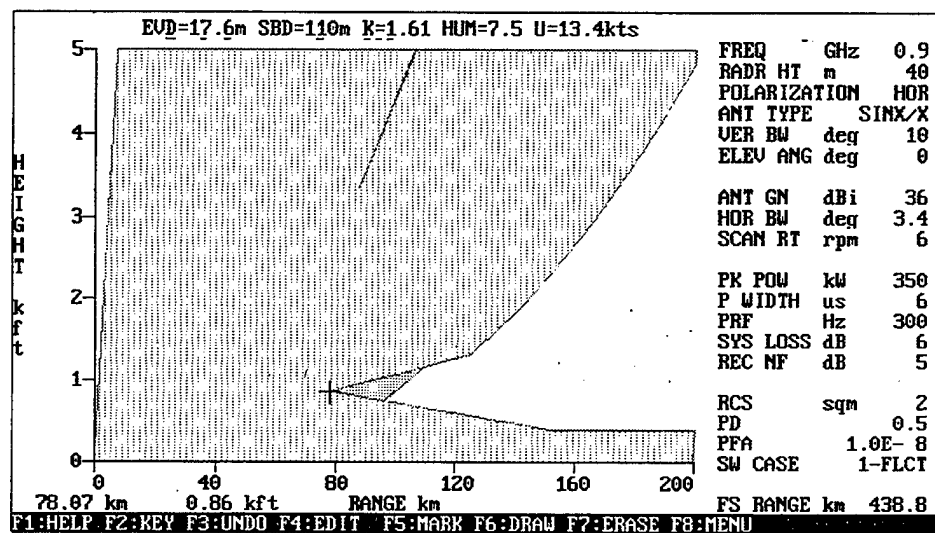


Figure 23. COVER output for SPS-49 radar, Antigua zone.

Figure 24 represents the PROPR output for the Sea Tiger radar operating in Antigua. The DD without ducting conditions was 61.7 km, and 70.8 km with ducting conditions. These results produce a DD difference of 9.1 km.

Figure 25 corresponds to PROPR output for RAN-10S radar with the Antigua zone conditions. It gives a DD of 63.4 km when there are no

ducting conditions, but 73.3 km when ducts are present, a DD difference of 9.9 km.

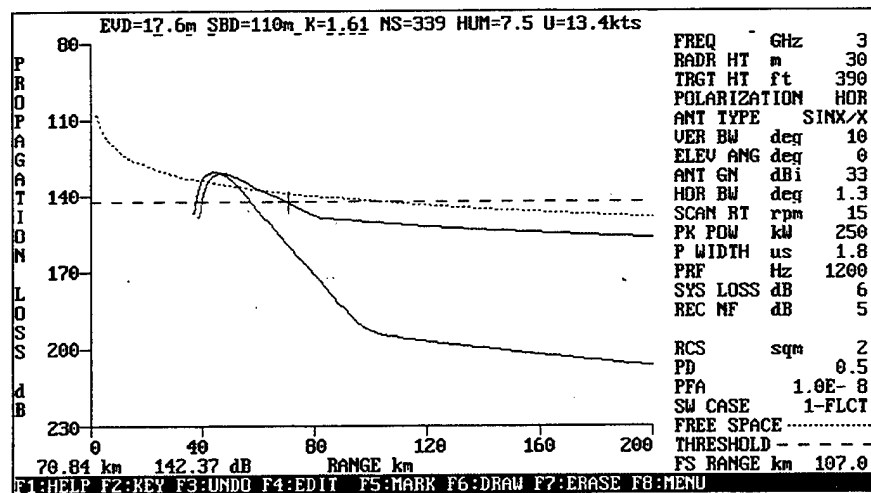


Figure 24. PROPR output for Sea Tiger radar, Antigua zone.

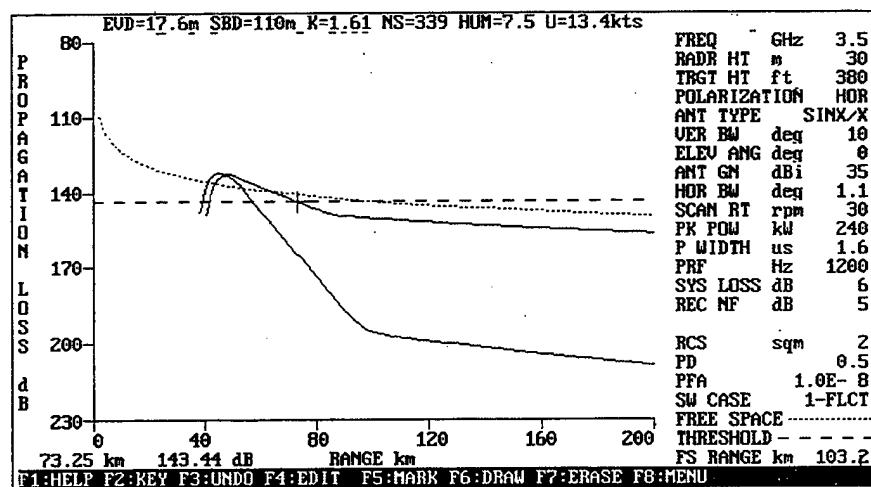


Figure 25. PROPR output for RAN-10S radar, Antigua zone.

Figure 26 represents PROPR output for SPS-49, it gives a DD of 87.2 km if there are no ducts, and 94.5 km for ducting conditions, producing a DD difference of 7.3 km.

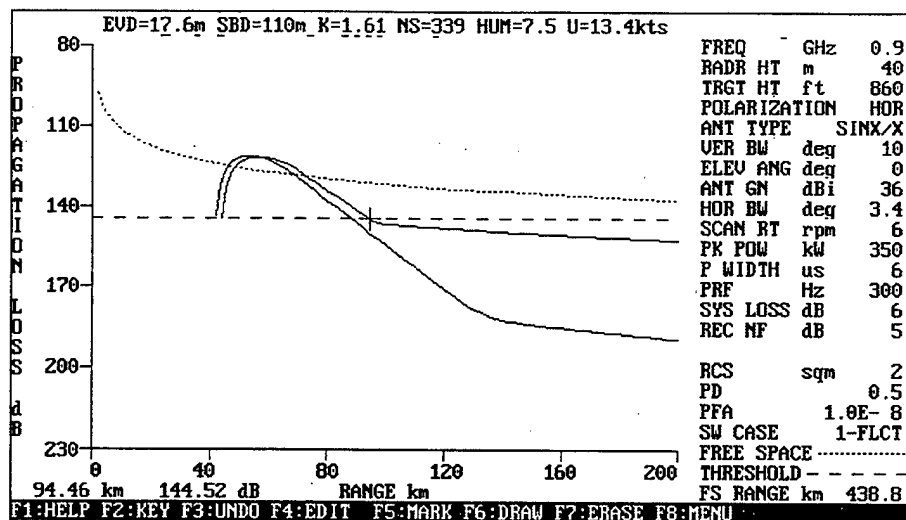


Figure 26. PROPR output for SPS-49 radar, Antigua zone.

Table 9 shows the Detection Distance difference between values given by COVER and PROPR when comparing ship-based radars with the data for conditions in the Antigua zone.

PROGRAMS	RADAR	DD no ducts	DD with ducts	DD Difference
COVER	Sea Tiger	63	77	14
	RAN-10S	64	76.6	12.6
	SPS-49	101	78	23
PROPR	Sea Tiger	58	70	12
	RAN-10S	57.8	73.3	15.5
	SPS-49	88.7	94.5	5.8

Table 9. Detection Distance Summary, Antigua zone.

2. Jamaica Zone

The Jamaica zone consists of two radiosonde stations. Kingston (WMOID 78397) located in Jamaica, and Guantanamo (WMOID 78367) located in Cuba. This zone was analyzed by using COVER with data from SDS, as shown in Figure 27, and the specifications of selected ship-mounted radars given in Table 6. COVER gave the output shown in Figure 28 for Sea Tiger, Figure 29 for RAN-10S, and Figure 30 for SPS-49.

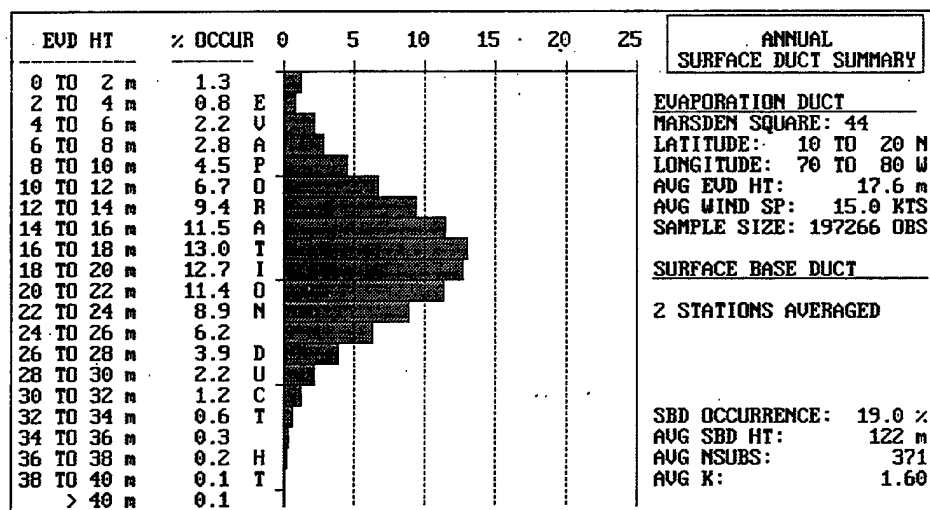


Figure 27. Evaporation Ducts Summary, Jamaica zone.

Figure 28 shows that the OAAD for the Sea Tiger radar is 410 feet, and a DD of 88.8 km with ducting conditions, and a DD of 65 km with

no ducts. If an aircraft is flying at an altitude of 1000 ft, the DD should be 99 km when ducting conditions are present, and 84 km if there are no ducts. This results in a DD difference of 14 km.

Figure 29 shows the COVER output for RAN-10S radar with Jamaica conditions. Here, an OAAD of 410 feet, at 76.1 km can be observed for ducting conditions, and 67 km for no ducts. Also, an aircraft at 1000 feet should be detected at 84 km in an environment with no ducts, and at 102 km with ducts. This results in a detection distance difference of 18 km.

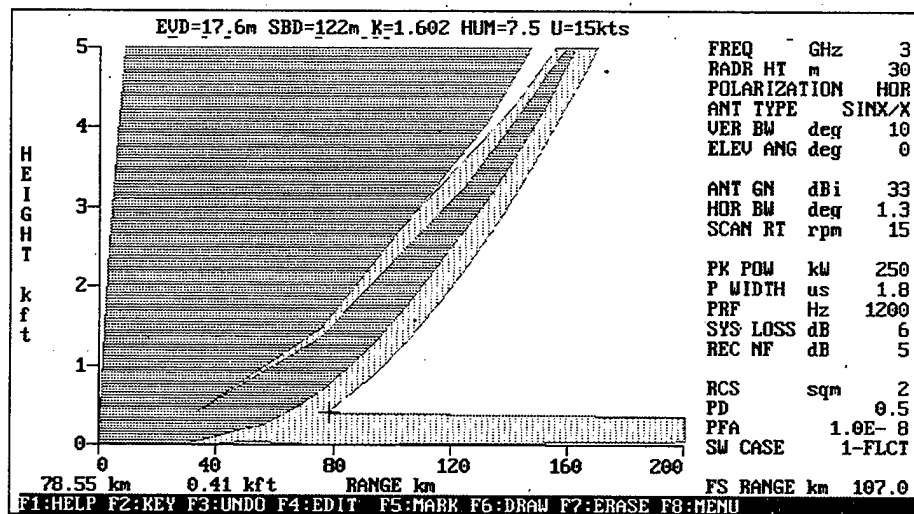


Figure 28. COVER output for Sea Tiger radar, Jamaica zone.

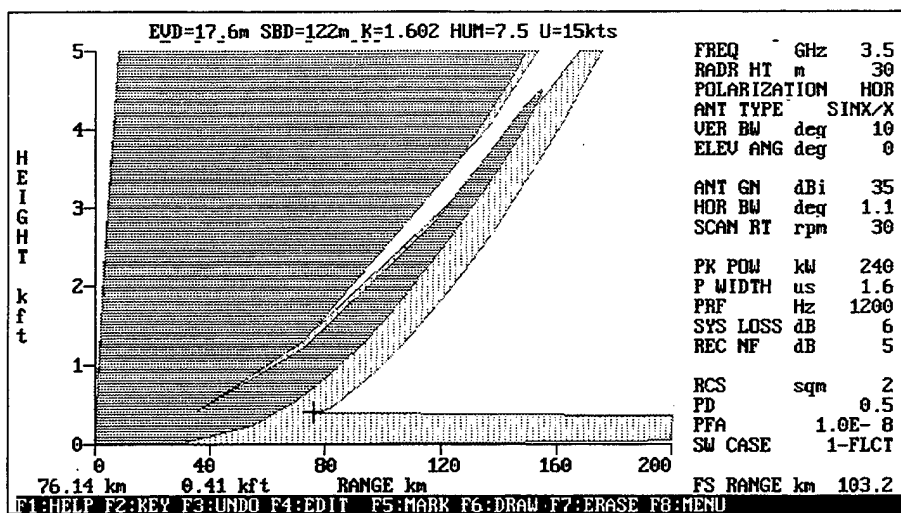


Figure 29. COVER output for RAN-10S, Jamaica zone.

Figure 30 corresponds to the COVER output for an SPS-49 with the Jamaica zone conditions. An OAAD of 900 feet, at 110.8 kilometers can be observed for ducting conditions, and a DD of 104 km for no ducts. For an aircraft at 1000 feet, this is a DD of 107 km in an environment with no ducts, and at 116 km with ducts, with a DD difference of 19 km.

Figure 31 represents the PROPR output for Sea Tiger operating in Jamaica. DD without duct conditions was 57.1 km, and 69.1 km with ducting conditions. These results produce a DD difference of 12 km.

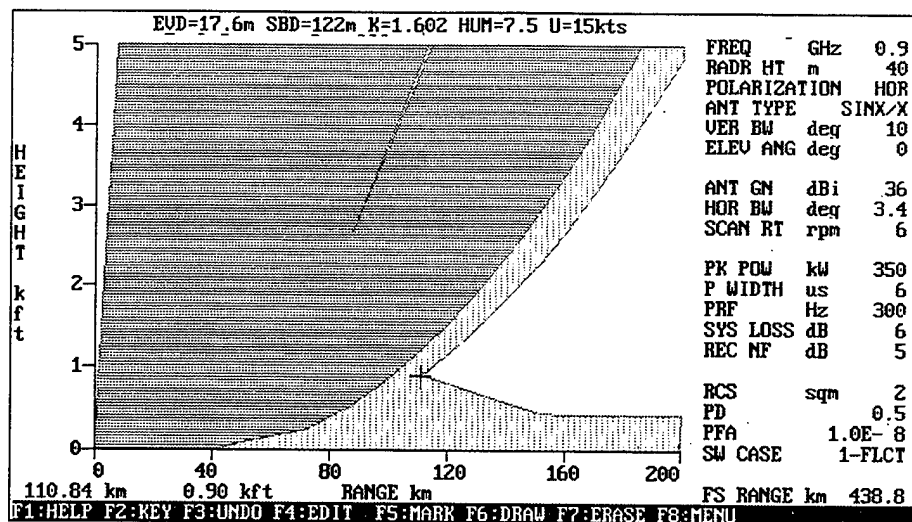


Figure 30. COVER output for SPS-49 radar, Jamaica zone.

Figure 32 is a presentation of the PROPR output for RAN-10S with the Jamaica zone conditions. The simulation gives a DD of 61.7 km when there are no ducting conditions, 74.2 km when ducts are present, with a DD difference of 12.5 km.

Figure 33, which represents PROPR output for SPS-49, gives a DD of 87.9 km if there are no ducts, and 95.4 km for ducting conditions, producing a DD difference of 7.5 km.

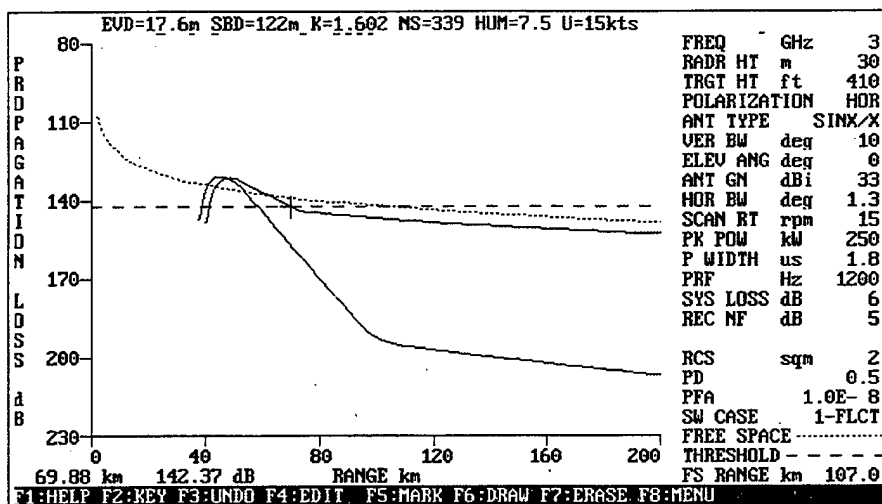


Figure 31. PROPR output for Sea Tiger radar, Jamaica zone.

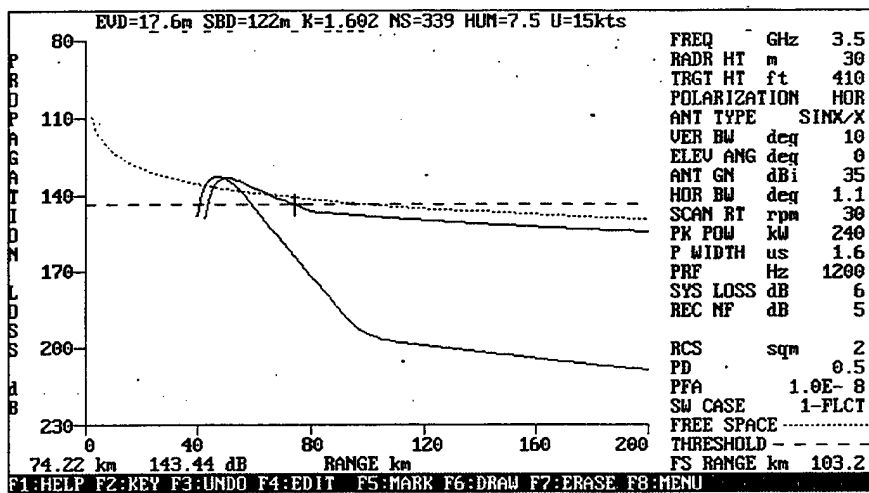


Figure 32. PROPR output for RAN-10S radar, Jamaica zone.

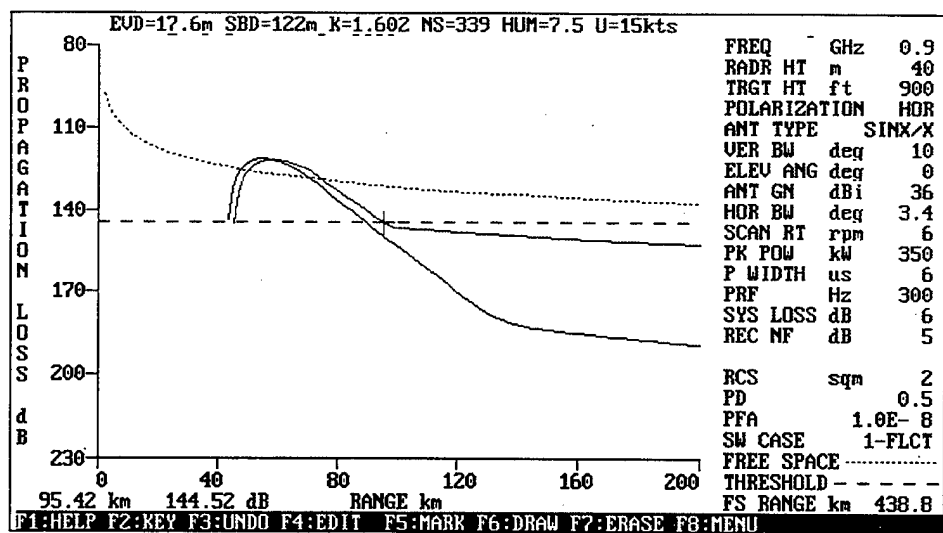


Figure 33. PROPR output for SPS-49 radar, Jamaica zone.

Table 10 shows the Detection Distance difference between values given by COVER and PROPR when comparing ship-mounted radars with the data for conditions in the Jamaica zone.

PROGRAMS	RADAR	DD no ducts	DD with ducts	DD Difference
COVER	Sea Tiger	65	78.6	13.6
	RAN-10S	67	76.1	9.1
	SPS-49	104	110.8	6.8
PROPR	Sea Tiger	58.3	69.9	11.6
	RAN-10S	59	74.2	15.2
	SPS-49	90.1	95.4	5.3

Table 10. Detection Distance Summary, Jamaica zone.

3. Puerto Rico Zone

The Puerto Rico zone consists of three radiosonde stations. Juliana (WMOID 78866) located in Saint Martin, San Juan (WMOID 78526) located in Puerto Rico, and Santo Domingo (WMOID 78486) located in Dominican Republic. This zone was analyzed by using COVER with data from SDS, as given in Figure 34, and same specifications of selected ship-based radars given in Table 6.

COVER gave the output given in Figure 35 for Sea Tiger, Figure 36 for RAN-10S, and Figure 37 for SPS-49.

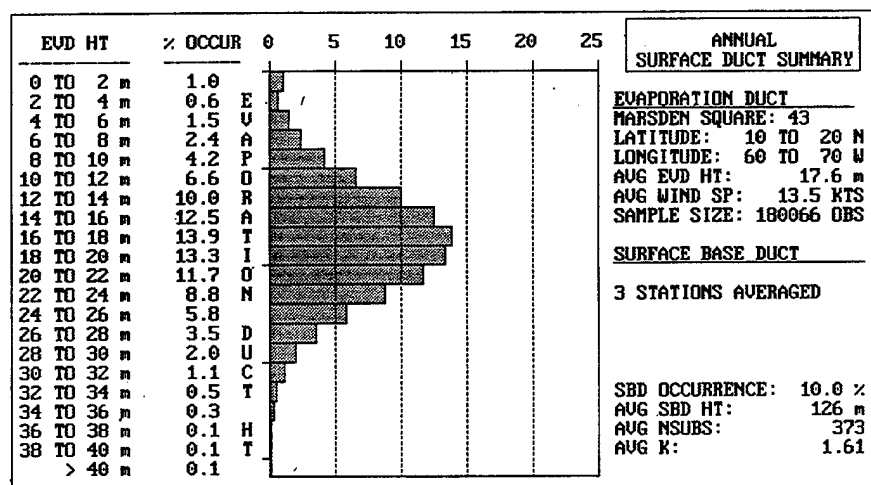


Figure 34. Evaporation Ducts Summary, Puerto Rico zone.

Figure 35 shows an OAAD for Sea Tiger radar of 430 feet, and a DD of 79.04 km with ducting conditions, and a DD of 67 km for no ducts. If an aircraft is flying at an altitude of 1000 ft, the DD should be

99 km when there are ducts, and 84 km if there are no ducts. This results in a DD difference of 15 km.

Figure 36 shows the COVER output for RAN-10S radar with Puerto Rico conditions. Here, an OAAD of 410 feet, at 80 km can be observed for ducting conditions, and 67 km for no ducts. Also, an aircraft at 1000 feet should be detected at 84 km in an environment with no ducts, and at 103 km with ducts, which results in a DD difference of 19 km.

Figure 37 shows the COVER output for the SPS-49 with the Puerto Rico zone conditions. An OAAD of 910 feet, at 112.3 kilometers can be observed for ducting conditions, and a DD of 107 km for no ducts. For an aircraft at 1000 feet, this is a DD of 104 km in an environment with no ducts, and 116 km with ducts, with a DD difference of 12 km.

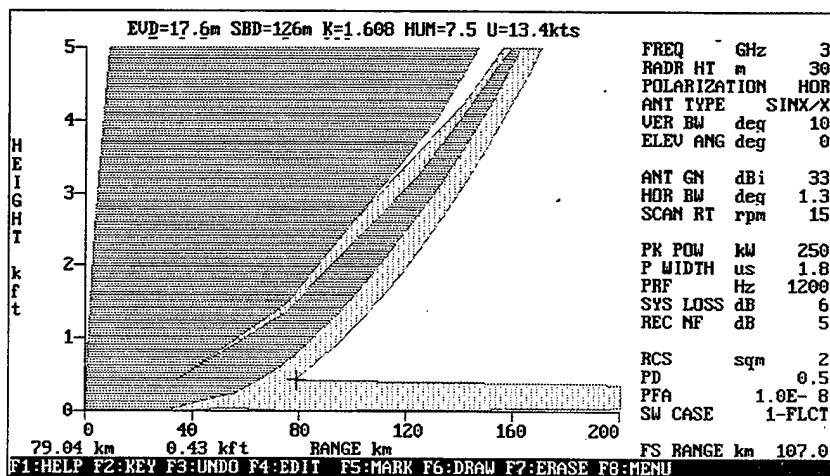


Figure 35. COVER output for Sea Tiger radar, Puerto Rico Zone.

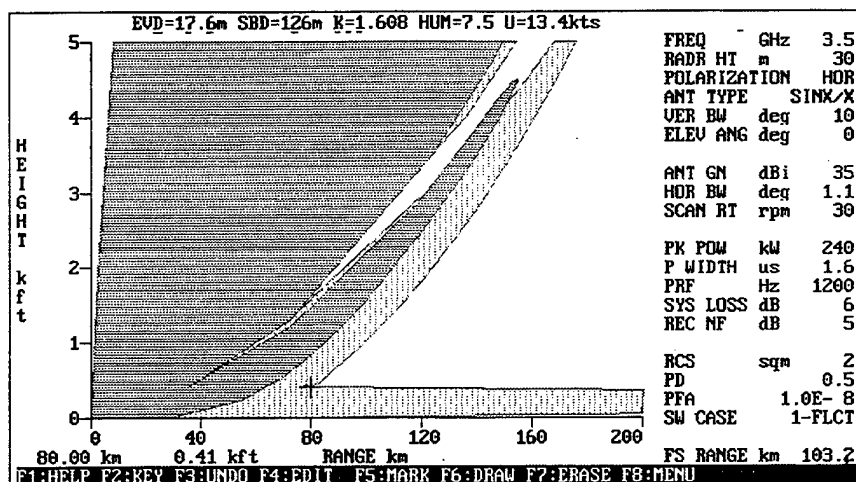


Figure 36. COVER output for RAN-10S, Puerto Rico zone.

Figure 37 shows the COVER output for the SPS-49 with the Puerto Rico zone conditions. An OAAD of 910 feet, at 112.3 kilometers can be observed for ducting conditions, and a DD of 107 km for no ducts. For an aircraft at 1000 feet, this is a DD of 104 km in an environment with no ducts, and 116 km with ducts, with a DD difference of 12 km.

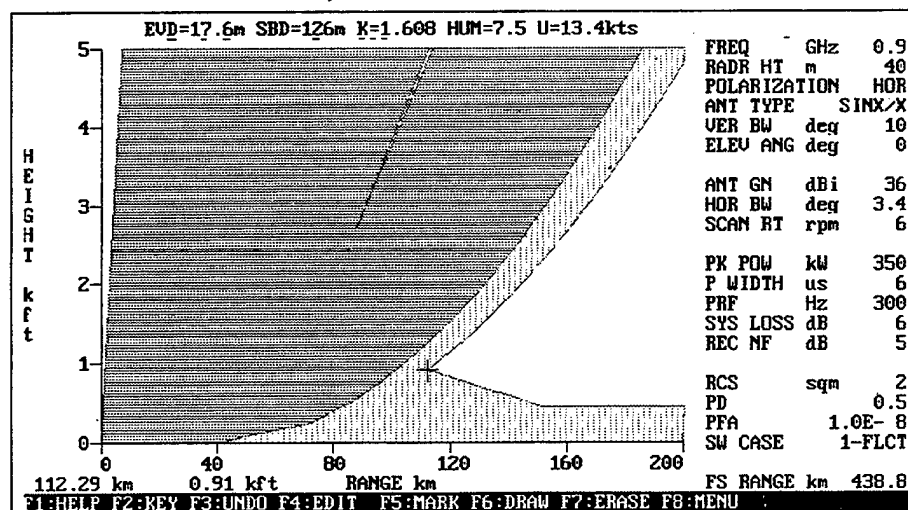


Figure 37. COVER output for SPS-49 radar, Puerto Rico zone.

Figure 38 represents the PROPR output for Sea Tiger operating in Puerto Rico. The DD without duct conditions was 63.1 km, and 72.39 km with ducting conditions. These results produce a DD difference of 9.29 km.

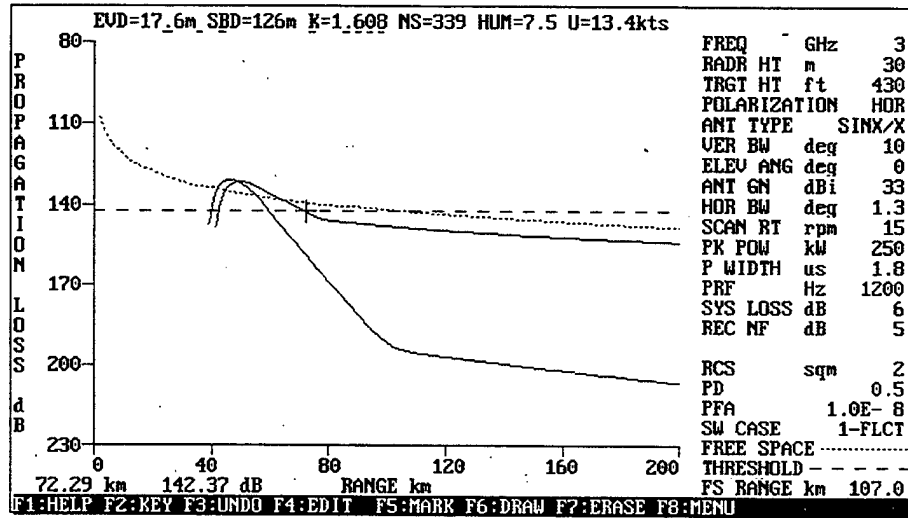


Figure 38. PROPR output for Sea Tiger radar, Puerto Rico zone.

Figure 39, which corresponds to PROPR output for RAN-10S with the Puerto Rico zone conditions, gives a DD of 62.6 km when there are no ducts, and 81 km when ducts are present, with a DD difference of 18.4 km.

Figure 40 represents PROPR output for SPS-49, gives a DD of 89.1 km if there are no ducts, and 96.4 km for ducting conditions, producing a DD difference of 7.3 km.

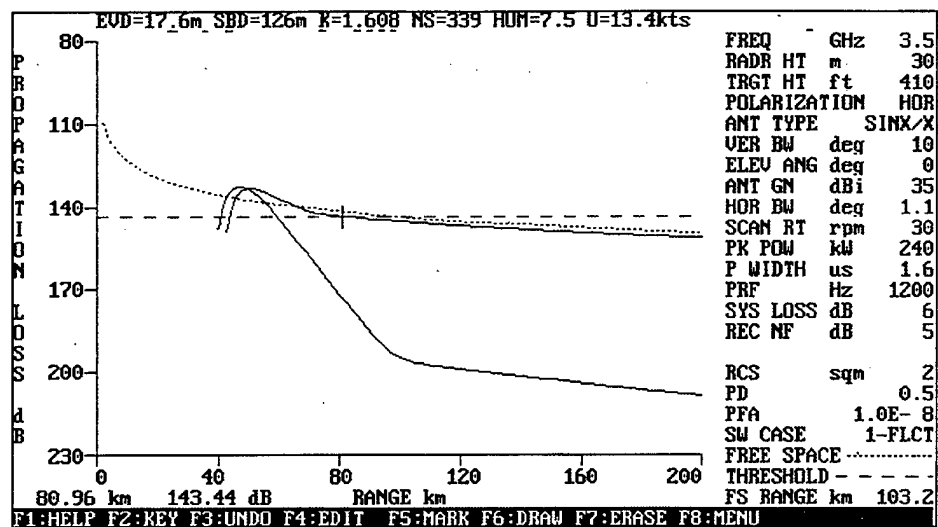


Figure 39. PROPR output for RAN-10S radar, Puerto Rico zone.

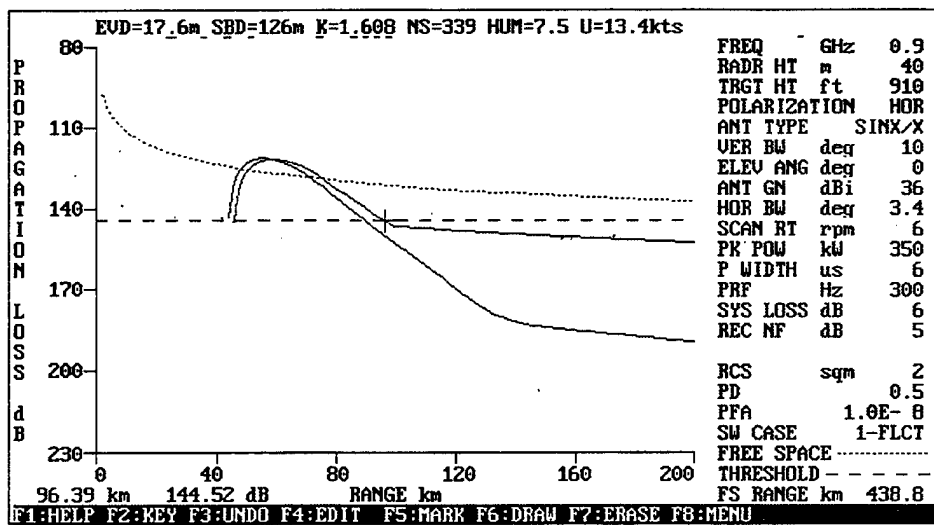


Figure 40. PROPR output for SPS-49 radar, Puerto Rico zone.

Table 11 shows the Detection Distance difference between values given by COVER and PROPR when comparing ship-mounted radars and data for conditions in the Puerto Rico zone.

PROGRAMS	RADAR	DD no ducts	DD with ducts	DD Difference
COVER	Sea Tiger	67	79	12
	RAN-10S	67	80	13
	SPS-49	107	112.3	5.3
PROPR	Sea Tiger	59.3	72.3	13
	RAN-10S	59	81	22
	SPS-49	89.6	96.4	6.8

Table 11. Detection Distance Summary, Puerto Rico zone.

C. SUMMARY OF RESULTS

In section B the results are very similar to those obtained for the land-based radars in section A. When comparing outputs given by COVER and PROPR, in section B, it can be seen that the detection distances and detection distance differences may differ from one program to another for the same analyzed radar systems. As noted before, these slight differences are due to the fact that COVER and PROPR use different assumptions for calculating propagation. However, the results

taken from PROPR are considered to be more accurate for all geometries [Ref. 1].

D. CONSIDERATIONS FOR TACTICAL DATA COLLECTION

In this section both percent occurrence of surface-based ducts and data collection are addressed. First of all, it can be seen from SDS outputs that percent of occurrence of surface-based ducts varies from low values of 3% to medium values of 19%. Second, due to the high impact of the atmosphere on the propagation of electromagnetic waves, it is important to collect data as close as possible to the place where military operations are being carried out, and in real time, in order to assure accurate data.

1. Percent of Occurrence of Evaporation Ducts

The evaporation height distribution given by SDS shows that the evaporation ducting effects in all of the radiosonde stations located in MS 43 and 44 are quite strong. Above 12 meters the percent of occurrence is

more than 60% in all the stations located in the area of interest. Table 12 shows both the SBD occurrence and the SBD heights in the whole area.

Radiosonde Station Zones	SBD occurrence	SBD Height
Curacao	3.0 %	88 m
Trinidad and Tobago	12.5 %	120 m
Antigua	6 %	110.5 m
Jamaica	19 %	121.5 m
Puerto Rico	10 %	125.67 m

Table 12. SBD occurrence and heights for MS 43 and 44.

As shown in Table 12, the Evaporation Duct occurrence may vary from very low values like 3.0 % in the Curacao zone, to medium values like 19 % in Jamaica. On the other hand, the average SBD heights vary from 88 m in Curacao to almost 126 m in Puerto Rico. This last situation produces different optimal altitudes to avoid detection for the same radar in different zones, as seen in sections A and B.

On the other hand, percent SBD occurrence creates the need for exact and timely tactical data about the operation area. This is due to the fact that most of the data comes from stations and/or ships located far away from the area of operations. Likewise, these data are collected at different times of the day from when the operations are going to be

carried out. It is quite important to collect data from the area of the operations in a timely manner. One of the means to collect tactical climatological data is the use of TDROP.

2. Enhancements in Tactical Data Collection (Tactical Dropsonde)

Although there are many radiosonde stations located around the world, and radiosonde ships navigate in every ocean, data can almost never be collected close enough to the battlefield. Tactical decision aids rely on both accurate and timely data, so to enhance the operational performance of sophisticated sensor and weapon systems, accurate and near real-time data is needed.

Several R&D programs are examining approaches to obtain vertical profiles of refractivity in timely and accurate manners. Most involve an aircraft mounted or deployed sensor. The aircraft range from various sizes of Unmanned Air Vehicles (UAV) to various types of piloted operational jet and non-jet aircraft. The in situ sensors are attached to the UAV or are sondes that are deployed and descend under a parachute versus ascend with a balloon as with a shipboard sensor. Remote sensors are optical, e.g. LIDAR or interferometer, and are based on the interaction of water vapor amount and molecular temperature with the optical energy of given wavelength. Because this study has focused on

refractive effects on operations by tactical jets and because the preliminary stage of remote sensing methods, the examination was directed toward a sensor that can be deployed from an aircraft traveling at high speeds.

Tactical Dropsonde is a response from some organizations to solve the problem of precise real-time data collection from the battlefield. TDROP is designed to provide accurate temperature/moisture profile over the area of operations, and to transmit these data via real time RF link to serve as environmental input for tactical decision aids [Ref. 14].

TDROP is an electronic device which fits in USN AN/ALE-39 and/or AN/ALE-47 Countermeasures Dispenser Systems (CMDS). This electronic device has the function of acquiring pressure, humidity and temperature from the atmosphere. Data is transmitted via a real time RF link where it is used as input for tactical decision aids. Some TDROP may even use a GPS receiver to derive wind speed and direction data.

TDROP must overcome very demanding requirements, not only physical, but also operational to be used successfully in military operations. The TDROP must endure very high g-accelerations after being ejected from the aircraft, and while descending must acquire and transmit the atmospheric data. More detailed information about

Parameter	Performance Required
Ejection & Operation altitude	USN/USAF < 25,000 ft
Captive Carriage/ Non-operating	A/C Limits
Ejection Airspeed	< 450 KIAS
Ejection Velocity	> 100 ft/sec
Parachute Descent Rate	15 feet/sec @ 5 Kft
Transmit Frequency Range	131-173.5 Mhz
Transmit Range Line-of-sight	75 Nmi
Transmitted Data Encoding Tech	Manchester Encode, Serial ASCII
Operating Life	> 30 Minutes (Continuous)
CMDS Compatibility	AN/ALE-40, -47
Temperature Extremes	-40° C to +71° C
Payload Wt. (with parachute)	< 0.4 lb.

Table 13. Operational and Physical requirements for TDROP.

VI. CONCLUSIONS

Atmospheric refractive ducts which are present about 3 to 19% of the time in the south of the Caribbean Sea (depending on season and radiosonde station location) have a strong influence on the EM wave propagation of the selected land-based and ship-mounted radars. In this thesis the computer programs COVER and PROPR were used to predict the detection ranges of aircraft flying against selected radars. The most obvious effect of the ducts is an extended radar horizon resulting in an increase in radar coverage. Likewise, ducts are tactically very significant for an attacking aircraft attempting to penetrate a hostile environment. The approaching aircraft can possibly delay or avoid detection by flying over the ducts.

Statistical and historical data taken from radiosonde stations are designed for synoptic weather analysis and are not precise enough to draw conclusions that can be used in tactical applications. New and enhanced methods for tactical data collection are required. Consequently the TDROP was conceived to collect accurate and timely tactical climatological data. After being ejected from the existing CMDS, TDROP must gather and transmit meteorological data in real time. Data can be

used as input for other tactical decision aid programs like EREPS and EOTDA.

LIST OF REFERENCES

1. Patterson, W. L., et al, *Engineer's Refractive Effects Prediction System (EREPS) Revision 3.0*, Technical Document, NCCOSC, 1994.
2. Hess, S. L., *Introduction to Theoretical Meteorology*, Holt, Rinehart and Winston, New York, 1959.
3. Andrade, A. C. A., *Mesoscale Variability of the Caribbean Sea from GEOSAT*, M. S. Thesis, Naval Postgraduate School, Monterey, 1991.
4. Davidson, K., *Meteorology for EW*, Class Notes, 1997.
5. Gaviria, M., *Assessment of the Effects of Refractive Conditions on Electronic Warfare in Central America*, M.S. Thesis, Naval Postgraduate School, Monterey, 1990.
6. Collin, R., *Antennas and Radiowave Propagation*, Mc Graw-Hill. New York, 1985.
7. Rangel, R., *Comint Analysis in a Littoral Environment*. M.S. Thesis, Naval Postgraduate School, Monterey, 1996.
8. Fitts, R. E., *The Strategy of Electromagnetic Conflict*, Peninsula Publishing, CA, 1980.

9. Naval Air Systems Command, *Electronic Warfare and Radar Systems Engineering Handbook*, NAWC, 1997.
10. Skolnik M. I., *Introduction to Radar Systems*, McGraw-Hill, 1980
11. Neri, Filippo, *Introduction to Electronic Defense Systems*, Artech House Inc., Norwood, 1991.
12. Streetly, M., *Jane's Radar and Electronic Warfare Systems*, Jane's information Group Inc., Alexandria, 1998.
13. Tracor Aerospace Inc., *Performance Specification for the GPS Tactical Dropsonde and HiMetSonde*, Austin, 1998.
14. Frederickson, P., Davidson, K., et al, *Evaluation of the Tactical Dropsonde in the Coastal Environment*, SPAWAR, 1996.
15. Ahrens, C. D., *Meteorology Today*. West Publishing Company, New York, 1994.
16. Shumaker, David L., et al, *Infrared Imaging Systems Analysis*, The Environmental Research Institute of Michigan, 1993.

INITIAL DISTRIBUTION LIST

	No. Copies
1. Defense Technical Information Center..... 8725 John J. Kingman Rd. STE 0944 Ft. Belvoir, VA 22060-6218	2
2. Dudley Knox Library..... Naval Postgraduate School 411 Dyer Rd. Monterey, CA 93943-5101	2
3. Professor Dan C. Boger, Chairman Code CS..... Naval Postgraduate School 833 Dyer Road Monterey, CA 93943-5118	1
4. Professor K. L. Davidson, Code MR/DS..... Naval Postgraduate School 833 Dyer Road Monterey, CA 93943-5100	5
5. Professor D. Jenn, Code EC/JN..... Naval Postgraduate School 833 Dyer Road Monterey, CA 93943-5100	1
6. G/D Gil Humberto Reyes Sarrameda Comandante General de la Aviación COGEAVIA, La Carlota BAGEM Caracas, DF Venezuela	1
7. G/B Arturo Jose Garcia Comandante de Personal COGEAVIA, La Carlota BAGEM Caracas, DF Venezuela	1
8. G/B Agregado Aéreo..... Embassy of Venezuela 2409 California Street N.W. Washington, DC 20008	1